Int. J. Solids Structures, Vol. 18, No. 6, pp. 497–531, 1982
Printed in Great Britain.

0020-7683/82/060497-35$03.00/0
Pergamon Press Ltd.

A PLASTICITY MODEL FOR FLOW OF GRANULAR MATERIALS UNDER TRIAXIAL STRESS STATES

J. F. DORRIS† and S. NEMAT-NASSER
Northwestern University, Evanston, IL 60201, U.S.A.

(*Received* 20 *January* 1981; *in revised form* 12 *August* 1981)

Abstract—For finite deformations of granular materials, a plasticity theory is developed which accounts for the true stress triaxiality, pressure sensitivity and dilatancy. The effect of stress triaxiality is introduced by including the third deviatoric stress invariant in the yield function and the flow potential. For illustration, the true triaxial test on a cubical sample is analyzed in detail, the results are compared with experimental observations of true triaxial tests on loose and dense samples of sand, and good correlation is obtained.

1. INTRODUCTION

The Coulomb failure criterion asserts that a granular mass remains rigid until the shear stress, τ, on any plane reaches a critical value,

$$|\tau| = c_o + \sigma \tan \phi, \tag{1.1}$$

where c_0 is the cohesive strength, σ is the normal compressive stress acting on the plane, and ϕ is the angle of friction. Once this critical value is reached, the granular mass is regarded to slip as two rigid bodies along the plane which transmits the critical shear stress.

Mohr has generalized this hypothesis by stating that shear failure occurs along the plane on which the shear and normal stresses are related by a specific relation,

$$|\tau| = f(\sigma). \tag{1.2}$$

The function f is constructed experimentally by plotting Mohr's circles of stress for a series of tests with different confining pressures. The failure states then trace out a failure envelope in the τ, σ-plane. If the failure envelope is linear, the Mohr hypothesis reduces to the Coulomb criterion. For a cohesionless granular material ($c_o = 0$), the Mohr–Coulomb criterion can be written in terms of the principal stresses, $\sigma_1 \geq \sigma_2 \geq \sigma_3$ (compression is positive), as

$$\sin \phi = \frac{\sigma_1 - \sigma_3}{\sigma_1 + \sigma_3}. \tag{1.3}$$

It is apparent from this equation that the shear strength, as expressed by the angle of friction ϕ, is regarded to be independent of the intermediate principal stress, σ_2.

In many applications it is necessary to have knowledge of the deformation which precedes failure. To this end Drucker and Prager [1] have developed a plasticity theory which utilizes the Mohr–Coulomb criterion as a yield function and plastic potential. Kirkpatrick [2] has performed a series of experiments to establish an experimental yield surface. He then has compared this surface with the Mohr–Coulomb yield surface and pressure sensitive Tresca and von Mises yield surfaces, and has found the Mohr–Coulomb surface to be the most compatible with experimental observation. Since then the Mohr–Coulomb criterion has been generally employed as the yield surface for plasticity theories describing granular materials.

Experimental evidence, however, does not completely confirm the Mohr–Coulomb theory to be the correct yield surface. The most common tests used to study the yielding of granular materials are:

(1) Conventional triaxial compression test ($\sigma_1 > \sigma_2 = \sigma_3$), in which a cylinder with a lateral confining pressure $\sigma_l = \sigma_2 = \sigma_3$ and axial pressure $\sigma_a = \sigma_1$ is stressed to failure;

†Present address: Production Operations, Research Dept., Shell Development Company, Bellaire Research Center, P.O. Box 481, Houston, TX 77001, U.S.A.

(2) Conventional triaxial extension test ($\sigma_1 = \sigma_2 > \sigma_3$), in which a cylinder with a lateral confining pressure, $\sigma_l = \sigma_1 = \sigma_2$, and axial pressure, $\sigma_a = \sigma_3$, is stressed to failure;

(3) Plane strain test, ($\sigma_1 > \sigma_2 > \sigma_3$).

Of the three tests only the compression test agrees with the predictions of the Mohr–Coulomb theory which underestimates the results observed in the extension and plane strain tests.

The results from the plane strain tests indicate that there is a dependence of the shear strength on the intermediate principal stress in contradiction to the Mohr–Coulomb theory. Since in general practice the state of stress is usually triaxial, it is of fundamental interest to know the shear strength characteristics over the whole range of σ_2, $\sigma_1 \geq \sigma_2 \geq \sigma_3$.

This problem has been approached by a number of experimentalists who have studied the true triaxial states of stress by loading opposite faces of cubical samples with three unequal principal stresses. Some of the more recent experimental investigations have been done by Arthur *et al.*[3], Lade and Duncan[4], Reades and Green[5], and Sutherland and Mesdary[6]. The results of the true triaxial tests are usually presented by plotting the angle of friction as a function of the dimensionless parameter, $b = (\sigma_2 - \sigma_3/\sigma_1 - \sigma_3)$, which is a measure of stress triaxiality and is limited to the range $0 \leq b \leq 1$. The value of $b = 0$ corresponds to the conventional triaxial compression test, $b = 1$ corresponds to the conventional triaxial extension test, and b is in the range $0.2 \leq b \leq 0.4$ for the plane strain test. The results presented in[3–6] are summarized in Fig. 1. From this figure it is clear that the experimentalists agree that the shear strength should increase with increasing b, up to the plane strain value of b. However above the plane strain value of b, there is no general agreement about how the strength should vary. In particular there is disagreement about the sign of $(d\phi/db)$ as $b \to 1$ and about the magnitude of the strength at $b = 1$. There are of course many other investigators who should be mentioned in relation to the results presented in Fig. 1. The information given in this figure, however, is representative of the type of results observed for values of b beyond the plane strain values. The reader should refer to Green[7] for references to other triaxial tests.

It appears that the controversy over the test results can be attributed to the type of triaxial apparatus employed. The need to independently apply three unequal principal stresses on a cubical sample while maintaining a homogeneous deformation, presents considerable mechanical difficulties. The previously mentioned experimentalists have utilized designs that load the faces of the cubical sample with various combinations of pressurized membranes and rigid platens. Each method of loading has its own disadvantages. The flexible membrane tends to

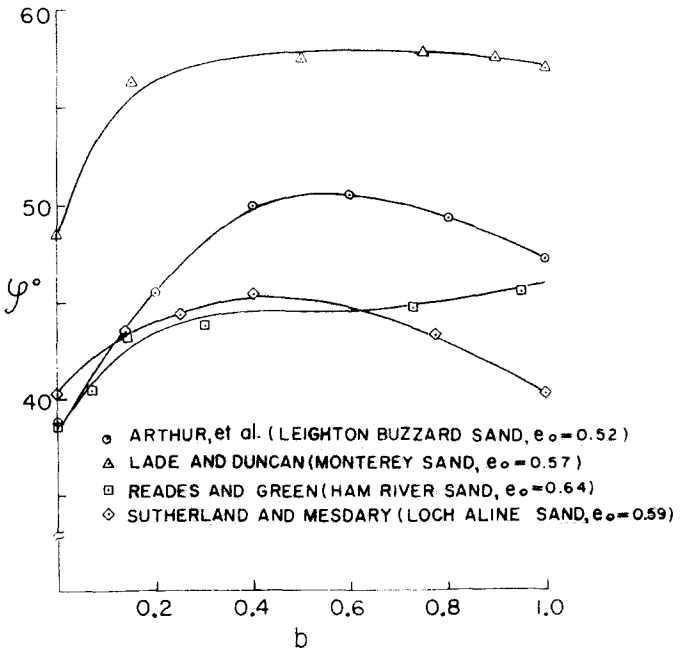

Fig. 1. Variation of the angle of friction, ϕ, with b; Experimental results are from Arthur *et al.*[3], Lade and Duncan[4], Reades and Green[5] and Sutherland and Mesdary[6].

induce inhomogeneous deformations along the edges of the sample, while the friction from the rigid platens creates shear stresses on the faces of the sample. Because of these problems there are some doubts about the interpretation of the results.

In order to accurately describe the behavior of granular materials, it is necessary to allow for the effects of inelastic volume changes, pressure sensitivity, and internal friction. Nemat-Nasser and Shokooh[8] have proposed a plasticity theory with a non-associated flow rule that systematically modifies the usual J_2-flow potential and yield function to include these effects. Their theory which allows for finite deformations is a generalization of a number of recently developed specialized plasticity theories and contains the essential features of critical state soil mechanics. They have applied their theory to predict experimental results of conventional triaxial tests of crushed granite and Ottawa sand with good correlation. However their theory is only applicable to two-dimensional states of stress. By introducing the third invariant of the stress deviator into the plastic potential and yield function, the results of Nemat-Nasser and Shokooh can be generalized for application to three-dimensional states of stress.

Here the behavior of granular materials has been discussed from the point of view of the Mohr–Coulomb failure (or yield) condition. There are, of course, other aspects of the mechanical behavior of granular masses, which are not examined here; see, e.g. [9–33]. Representative continuum theories based on concepts from classical plasticity such as yield surfaces, flow-potentials, etc. are developed by Lade[16], Mróz[20], Prevost[25], Romano[26], Schofield and Wroth[28], Vermeer[32] and Wilde[33]. Lade's [16] work includes nine parameters which can be derived from the results of conventional triaxial compression tests. The theory of Schofield and Wroth[28] describes plastic flow in terms of the critical states. The theory of Vermeer[32] divides the plastic strain into two parts: one part is described by a shear yield surface with a non-associated flow rule that includes Rowe's[27] stress dilatancy equation, and the other part includes inelastic volume strains. Wilde[33] proposes a theory with an associated flow rule based on extension of the usual J_2-plasticity theory. More recently a micromechanical approach has been proposed by Christoffersen *et al.*[10] which yields the results of the double-sliding flow theory of Spencer[30, 31] as a special case; see also Mehrabadi and Cowin[19]. A survey of the basic development in this area has been given by Mróz[34].

It should be kept in mind that the constitutive relations presented in this paper are not restricted to granular media. The mechanical behavior of other materials such as rocks and porous metals also exhibits inelastic volume changes, pressure sensitivity, and internal friction. Berg's[35] work pertains to small plastic deformation of microporous metal aggregates, and involves a pressure sensitive yield surface. Rudnicki and Rice[36] develop a theory to model the behavior of brittle rock masses which includes dilatancy and pressure sensitivity. The experimental results of Mogi[37] on cubical samples of rock show results similar to those observed in granular materials; for a discussion relating to high pressure and temperature, and other effects pertinent to geophysical applications, see[38].

2. FORMULATION

For simplicity, a fixed rectangular Cartesian coordinate system with coordinate axes, x_i, $i = 1, 2, 3$, is used. The material is regarded rate independent, and therefore the time parameter may be any convenient monotone quantity; this parameter is denoted by θ, and a superposed dot indicates material rate of change with respect to θ. The velocity field is v_i, and $D_{ij} = (1/2)(v_{i,j} + v_{j,i})$ denotes the rate of deformation tensor, where a comma followed by an index represents partial differentiation with respect to the corresponding coordinate. According to Hill[39], Mandel[40, 41] and Nemat-Nasser[42], the rate of deformation obeys an exact additive decomposition.

$$D_{ij} = D^e_{ij} + D^p_{ij}, \tag{2.1}$$

where superscript e denotes the contribution from the elastic deformation, and superscript p is that from the plastic part.

For problems of interest here, the elastic strain rate may be related to a (properly invariant) stress rate by means of a linear relation similar to Hooke's law. For example, with $\overset{*}{\sigma}_{ij}$ denoting

the Jaumann rate of change of the Cauchy stress,

$$\overset{*}{\sigma}_{ij} = \dot{\sigma}_{ij} - W_{ik}\sigma_{kj} - W_{jk}\sigma_{ki}, \quad i = 1, 2, 3, \tag{2.2}$$

it may be assumed that

$$D^e_{ij} = \frac{\overset{*}{\sigma}'_{ij}}{2\mu}, \quad D^e_{kk} = \frac{\overset{*}{\sigma}_{kk}}{3\kappa}, \tag{2.3}$$

where repeated indices are summed, prime denotes the deviatoric part, μ is the shear modulus, and κ is the bulk modulus; in (2.2), $W_{ij} = (1/2)(v_{i,j} - v_{j,i})$ is the spin tensor. Of course an anisotropic relation of the form $D^e_{ij} = D_{ijkl}\overset{*}{\sigma}_{kl}$, where D_{ijkl} is the elastic compliance, may be more appropriate. The plastic part of the deformation rate tensor is expressed in terms of a flow potential, g, as

$$D^p_{ij} = \dot{\lambda}\frac{\partial g}{\partial \sigma_{ij}}, \tag{2.4}$$

where σ_{ij} is the total stress (the deviatoric part plus the spherical part), and $\dot{\lambda}$ is a scalar function.

The yield function, f, and the plastic potential, g, are assumed to depend on the state of stress including the hydrostatic pressure (or tension), on the total *plastic* volumetric strain, Δ, measured with respect to a suitable reference state, and on the total distortional plastic work, ξ. The effect of the distortional stress and the hydrostatic pressure on the yield function and the flow potential is described by

$$\begin{aligned} f &\equiv J^{1/2}[1 + c(\eta)] - F(I, \Delta, \xi) \quad \text{(yield function)}, \\ g &\equiv J^{1/2}[1 + c(\eta)] + G(I, \Delta, \xi) \quad \text{(flow potential)}, \end{aligned} \tag{2.5}$$

where

$$\begin{gathered} I = \sigma_{ii}, \ \Delta = \int_0^\theta \frac{\rho_o}{\rho} D^p_{ii}\, \mathrm{d}\theta', \quad \xi = \int_0^\theta \frac{\rho_o}{\rho}\sigma'_{ij}D^p_{ij}\, \mathrm{d}\theta', \\ \eta = \frac{J_3}{J^{3/2}}, \ J = \frac{1}{2}\sigma'_{ij}\sigma'_{ij}, \quad J_3 = \frac{1}{3}\sigma'_{ij}\sigma'_{jk}\sigma'_{ki}; \end{gathered} \tag{2.6}$$

for simplicity in notation, J is used for the commonly used J_2, I for the commonly used I_1, and superscript p on Δ is deleted, although Δ represents the plastic part of the volumetric strain only. In (2.6), ρ_o and ρ are the mass density in the reference and in the current states, respectively. In applications where it is convenient to use the current configuration for reference, one sets $\rho_o = \rho$ *after* the integration in $(2.6)_{2,3}$ is performed. The term c in (2.5) is a function of the dimensionless stress ratio η. This function introduces the third stress invariant J_3 into the yield function and plastic potential, and can be viewed as a perturbation of the equations proposed by Nemat-Nasser and Shokooh [8].

If g is substituted into (2.4), the plastic part of the deformation rate tensor results,

$$D^p_{ij} = \dot{\lambda}\left\{\frac{1}{J}\frac{\partial c}{\partial \eta}\sigma'_{ik}\sigma'_{kj} + \left[\frac{1}{2J^{1/2}}(1 + c) - \frac{3}{2}\frac{J_3}{J^2}\frac{\partial c}{\partial \eta}\right]\sigma'_{ij} - \left(\frac{2}{3}\frac{\partial c}{\partial \eta} - \frac{\partial G}{\partial I}\right)\delta_{ij}\right\}. \tag{2.7}$$

The scalar function $\dot{\lambda}$ is determined from the consistency condition $\dot{f} = 0$, which yields

$$\dot{\lambda} = \frac{1}{H}\left\{(J^{1/2})^{\cdot}(1 + c) + J^{1/2}\dot{c} - \frac{\partial F}{\partial I}\dot{I}\right\}, \tag{2.8}$$

where

$$H = \frac{\rho_o}{\rho}\left\{3\frac{\partial G}{\partial I}\frac{\partial F}{\partial \Delta} + J^{1/2}(1+c)\frac{\partial F}{\partial \xi}\right\}. \tag{2.9}$$

Since

$$(J^{1/2})^{\cdot} = \frac{1}{2J^{1/2}}\sigma'_{ij}\overset{*}{\sigma}_{ij},\ \dot{I} = \overset{*}{\sigma}_{ii}, \text{ and}$$

$$\dot{c} = \frac{\partial c}{\partial \eta}\frac{\partial \eta}{\partial \sigma_{ij}}\overset{*}{\sigma}_{ij} = \frac{\partial c}{\partial \eta}\frac{1}{J^{3/2}}\left(\sigma'_{ik}\sigma'_{kj} - \frac{3}{2}\frac{J_3}{J}\sigma'_{ij} - \frac{2}{3}J\delta_{ij}\right)\overset{*}{\sigma}_{ij},$$

(2.4) and (2.8) yield

$$D^p_{ij} = \frac{1}{H}\left\{\frac{1}{J}\frac{\partial c}{\partial \eta}\sigma'_{in}\sigma'_{nj} + \left[\frac{1}{2J^{1/2}}(1+c) - \frac{3}{2}\frac{J_3}{J^2}\frac{\partial c}{\partial \eta}\right]\sigma'_{ij} - \frac{2}{3}\frac{\partial c}{\partial \eta}\delta_{ij}\right\}$$
$$\times\left\{\frac{1}{J}\frac{\partial c}{\partial \eta}\sigma'_{kn}\sigma'_{nl} + \left[\frac{1}{2J^{1/2}}(1+c) - \frac{3}{2}\frac{J_3}{J^2}\frac{\partial c}{\partial \eta}\right]\sigma'_{kl} - \left(\frac{2}{3}\frac{\partial c}{\partial \eta} + \frac{\partial F}{\partial I}\right)\delta_{kl}\right\}\overset{*}{\sigma}_{kl}, \tag{2.10}$$

$$D^p_{ii} = \frac{3}{H}\frac{\partial G}{\partial I}\left\{\frac{1}{J}\frac{\partial c}{\partial \eta}\sigma'_{ik}\sigma'_{kj} + \left[\frac{1}{2J^{1/2}}(1+c) - \frac{3}{2}\frac{J_3}{J^2}\frac{\partial c}{\partial \eta}\right]\sigma'_{ij} - \left(\frac{2}{3}\frac{\partial c}{\partial \eta} + \frac{\partial F}{\partial I}\right)\delta_{ij}\right\}\overset{*}{\sigma}_{ij}. \tag{2.11}$$

These equations hold as long as the yield condition, $f = J^{1/2}(1+c) - F = 0$, is satisfied.

Finally one may combine the plastic and elastic contributions to the total deformation rate from (2.11), (2.10), (2.3) and (2.1), to arrive at

$$D_{ij} = L_{ijkl}\overset{*}{\sigma}_{kl}, \tag{2.12}$$

where

$$L_{ijkl} = \frac{1}{4\mu}(\delta_{ik}\delta_{jl} + \delta_{jk}\delta_{il}) + \left(\frac{1}{9\kappa} - \frac{1}{6\mu}\right)\delta_{ij}\delta_{kl}$$
$$+ \frac{1}{H}\left\{A_2\sigma'_{in}\sigma'_{nj} + A_1\sigma'_{ij} - \left(A_o - \frac{\partial G}{\partial I}\right)\delta_{ij}\right\}$$
$$\times\left\{A_2\sigma'_{kn}\sigma'_{nl} + A_1\sigma'_{kl} - \left(A_o + \frac{\partial F}{\partial I}\right)\delta_{kl}\right\}, \tag{2.13}$$

$$A_2 = \frac{1}{J}\frac{\partial c}{\partial \eta}, \quad A_1 = \frac{1}{2J^{1/2}}(1+c) - \frac{3}{2}\frac{J_3}{J^2}\frac{\partial c}{\partial \eta}, \quad A_o = \frac{2}{3}\frac{\partial c}{\partial \eta}.$$

The inverse of (2.12) is

$$\overset{*}{\sigma}_{ij} = M_{ijkl}D_{kl}, \tag{2.14}$$

where

$$M_{ijkl} = \mu(\delta_{ki}\delta_{lj} + \delta_{kj}\delta_{li}) + \left(\kappa - \frac{2}{3}\mu\right)\delta_{ij}\delta_{kl}$$
$$-\left[H + \mu(1+c)^2 + \mu(4/3 - 9\eta^2)\left(\frac{\partial c}{\partial \eta}\right)^2 - 9\kappa\frac{\partial G}{\partial I}\frac{\partial F}{\partial I}\right]^{-1}$$
$$\times\left[2\mu A_2\sigma'_{in}\sigma'_{nj} + 2\mu A_1\sigma'_{ij} - \left(2\mu A_o - 3\kappa\frac{\partial G}{\partial I}\right)\delta_{ij}\right]$$
$$\times\left[2\mu A_2\sigma'_{kn}\sigma'_{nl} + 2\mu A_1\sigma'_{kl} - \left(2\mu A_o + 3\kappa\frac{\partial F}{\partial I}\right)\delta_{kl}\right]. \tag{2.15}$$

Equations (2.12)–(2.15) provide a complete set of constitutive relations for plastic materials in a general state of stress, whose response involves plastic volume changes and large plastic deformations, and that do not comply with the usual assumption of the associative flow rule.

In many experimental investigations of granular materials, the principal axes of stress and strain rate are not observed to coincide. To include this effect, one may take the plastic rate of deformation to be

$$D^p_{ij} = \dot{\lambda}\frac{\partial g}{\partial \sigma_{ij}} + \alpha\left(\overset{*}{\sigma}{}'_{ij} - \frac{1}{2J}\overset{*}{\sigma}_{kl}\sigma'_{kl}\sigma'_{ij}\right). \tag{2.16}$$

The second term on the right does not contribute to the rate of plastic work, and allows non-zero shear strain rates in the coordinate system coincident with the principal stress directions. The coefficient α is a scalar function of stress, strain, and strain history. The quantity $1/\alpha$ reduces to the secant modulus in the total deformation theory of Rudnicki and Rice[36], but in general it need not be interpreted in that manner. In fact, in the application to granular material behavior, α may even be negative, as in the double-sliding theory; see[19, 30, 31].

For $c = 0$, the equations of Nemat-Nasser and Shokooh[8] are easily recovered. The reader is referred to Nemat-Nasser and Shokooh for comparison to other plasticity theories.

3. CONSTITUTIVE PARAMETERS

When discussing the constitutive parameters developed in the preceding section it is necessary to establish a sign convention. Following the common practice in soil mechanics, compression and contraction are regarded positive and tension and extension negative.

From eqns (2.7)–(2.11) it is apparent that as far as the plastic potential is concerned, only $(\partial G/\partial I)$ appears in the constitutive relations. The quantity $(\partial G/\partial I)$ is calculated from (2.7),

$$3\frac{\partial G}{\partial I} = \frac{J^{1/2}(1+c)}{\sigma'_{ij}D^p_{ij}}D^p_{kk}. \tag{3.1}$$

Without loss in generality the function c is restricted so that $(1+c) > 0$. Since the denominator is always positive, the l.h.s. of (3.1) has the sign of D^p_{kk}. Hence $(\partial G/\partial I)$ is a measure of the instantaneous rate of plastic volumetric strain and is referred to as the "dilatancy factor".

By introducing the total effective plastic strain,

$$\gamma = \int_0^\theta (2D^{p'}_{ij}D^{p'}_{ij})^{1/2}\,\mathrm{d}\theta', \tag{3.2}$$

one can obtain a useful expression for $(\partial G/\partial I)$ which gives a clear physical interpretation of the dilatancy factor. First introduce

$$n_{ij} = \frac{1}{r}\frac{\partial g}{\partial \sigma'_{ij}}, \qquad r = \left(\frac{\partial g}{\partial \sigma'_{ij}}\frac{\partial g}{\partial \sigma'_{ij}}\right)^{1/2}, \tag{3.3}$$

where n_{ij} represents a unit measure in the deviatoric subspace, collinear with $D^{p'}_{ij}$. Then obtain

$$D^{p'}_{ij} = |D^{p'}_{ij}|n_{ij} = \frac{\dot{\gamma}}{r\sqrt{2}}\frac{\partial g}{\partial \sigma'_{ij}}. \tag{3.4}$$

Substituting (3.4) into (3.1), it follows that

$$3\frac{\partial G}{\partial I} = \frac{J^{1/2}(1+c)}{\dfrac{\dot{\gamma}}{r\sqrt{2}}\sigma'_{ij}\dfrac{\partial g}{\partial \sigma'_{ij}}}D^p_{kk} = \frac{r\sqrt{2}}{\dot{\gamma}}\frac{\dot{v}}{v} = \frac{r\sqrt{2}}{v}\frac{\mathrm{d}v}{\mathrm{d}\gamma}. \tag{3.5}$$

Here v denotes the current volume. Hence $(3/r\sqrt{2})(\partial G/\partial I)$ is the rate of volumetric strain,

$(\dot{v}/v)$, per unit rate of effective shear strain, $\dot{\gamma}$, and can be established experimentally. With the aid of $(2.6)_2$, (3.5) is written in terms of the total plastic volume strain,

$$\frac{d\Delta}{1-\Delta} = \frac{3}{r\sqrt{2}} \frac{\partial G}{\partial I} d\gamma. \tag{3.6}$$

Based on the commonly accepted assumption that a monotone and continuous shearing of cohesionless granular material leads to a critical void ratio, e_c, Nemat-Nasser and Shokooh[8] develop an equation relating $(\partial G/\partial I)$ to e_c and the initial void ratio, e_0. Following their reasoning one can establish a similar relation from (3.6),

$$\frac{3}{\sqrt{2}} \int_0^\infty \frac{1}{r} \frac{\partial G}{\partial I} d\gamma' = \ln\left(\frac{1+e_o}{1+e_c}\right), \tag{3.7}$$

which shows that there is a net amount of densification or dilatancy depending on whether $e_o > e_c$ (loose sand) or $e_o < e_c$ (dense sand). Figure 2 sketches the variation of the void ratio, e, with the strain, γ. Curve 1 is for loose sand $e_o > e_c$, for which e decreases monotonically with increasing γ, approaching e_c asymptotically. In this case $(\partial G/\partial I)$ remains positive (continuous densification). Curve 2 of Fig. 2, on the other hand, is for dense sand, $e_o < e_c$. In this case experiment shows that, similar to the case of loose sand, there is initial densification which is however followed by dilatancy. Hence $(\partial G/\partial I)$ is initially positive, but for dense sand, it becomes zero at a certain γ, and then is negative as γ is increased, approaching zero asymptotically. For this case there is always a net amount of dilatancy.

The yield function introduces three parameters, $(\partial F/\partial I)$, $(\partial F/\partial \xi)$ and $(\partial F/\partial \Delta)$. The quantity $(\partial F/\partial I)$ represents the sensitivity of material hardening to hydrostatic pressure. In this sense it represents the effect of internal friction on yielding of granular materials.

The work-hardening parameter, H, is seen to consist of two terms,

$$H = h_1 + h, \tag{3.8}$$

where

$$h_1 = 3\frac{\rho_o}{\rho} \frac{\partial G}{\partial I} \frac{\partial F}{\partial \Delta}, \qquad h = \frac{\rho_o}{\rho} J^{1/2}(1+c) \frac{\partial F}{\partial \xi}. \tag{3.9}$$

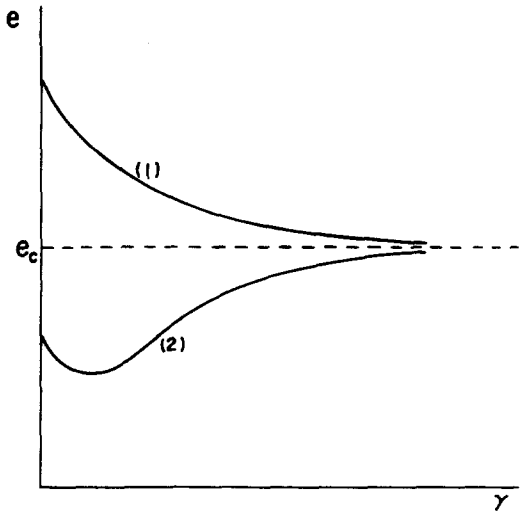

Fig. 2. Typical variation of the void ratio with effective strain for continuous monotonic shearing of a granular material; Curve 1 is for loose and Curve 2 is for dense materials.

First consider h. If one introduces the effective shear stress and the effective shear strain increment as

$$\tau = J^{1/2}, \quad \mathrm{d}\gamma = (2D_{ij}^{p\prime}D_{ij}^{p\prime})^{1/2}\,\mathrm{d}\theta, \tag{3.10}$$

then in a simple shear test the tangent to the shear stress–plastic strain curve is given by $h = (\mathrm{d}\tau/\mathrm{d}\gamma)$. For proportional loading and when $\rho_o \simeq \rho$, $J^{1/2}(\partial F/\partial\xi)$ is the tangent modulus, Hill[43]. For simple shear, h reduces to $h = (\rho_o/\rho)J^{1/2}(\partial F/\partial\xi)$ since $J_3 = 0$. Hence the quantity h measures work-hardening induced by plastic distortion.

The term h_1, on the other hand, corresponds to hardening (or softening) due to volumetric and pressure effects. For this reason one may refer to h_1 as the "density-hardening" parameter. In loose sands, e.g., only the density-hardening parameter seems to be of importance. It is observed that when $h = 0$, then $(\partial G/\partial I) = 0$ implies $H = 0$ and $D_{kk}^{p} = 0$. Moreover granular materials harden as they compact and soften as they dilate. Then from the sign convention it follows that $(\partial F/\partial\Delta) > 0$. Thus when $h = 0$, sign H = sign $(\partial G/\partial I)$, where sign stands for the sign function. It then follows that $H > 0$ implies $D_{kk}^{p} > 0$ (densification) and $H < 0$ implies $D_{kk}^{p} < 0$ (dilation), when $h = 0$. The critical state $(\partial G/\partial I) = D_{kk}^{p} = 0$ is defined when $H = 0$; see Section 4.

The functions F and G are seen to generate four constitutive parameters with clear physical interpretations, which account for inelastic volume changes, pressure sensitivity, and internal friction. The generality of F and G provides flexibility in adjustng the constitutive relations for specific applications. In the next section some simple but physically reasonable assumptions are made about these parameters, which allow us to test the preceding equations against results obtained in true triaxial tests of sand.

4. TRUE TRIAXIAL TEST

Again choose the sign convention of soil mechanics and let compression and contraction be positive, and tension and dilation negative. For the true triaxial test,

$$\sigma_{11} = \sigma_1 \geq \sigma_{22} = \sigma_2 \geq \sigma_{33} = \sigma_3 > 0, \quad \sigma_{ij} = 0 \text{ if } i \neq j. \tag{4.1}$$

To describe the influence of the intermediate principal stress, introduce the stress ratio b,

$$b = \frac{\sigma_2 - \sigma_3}{\sigma_1 - \sigma_3}. \tag{4.2}$$

Let the major stress difference be defined by

$$q = \sigma_1 - \sigma_3. \tag{4.3}$$

The components of the deviatoric stress tensor can now be written in terms of b and q as follows:

$$\sigma'_{11} = \frac{1}{3}(2-b)q, \quad \sigma'_{22} = \frac{1}{3}(2b-1)q, \quad \sigma'_{33} = -\frac{1}{3}(b+1)q, \quad \sigma'_{ij} = 0 \text{ if } i \neq j. \tag{4.4}$$

The invariants of the deviatoric stress tensor are

$$J = \frac{1}{2}\sigma'_{ij}\sigma'_{ij} = A^2q^2, \quad A^2 = \frac{1}{3}(b^2 - b + 1),$$

$$J_3 = \frac{1}{3}\sigma'_{ij}\sigma'_{jk}\sigma'_{ki} = B^3q^3, \quad B^3 = \frac{1}{27}(2b^3 - 3b^2 - 3b + 2). \tag{4.5}$$

For simplicity, assume

$$c(\eta) = \beta(b)\eta = \beta\frac{J_3}{J^{3/2}}. \tag{4.6}$$

Here β is a scalar which depends on the state of stress. The measure of distortion stress becomes

$$J^{1/2}(1+c(\eta)) = J^{1/2} + \beta\frac{J_3}{J} = K(b,\beta)q, \tag{4.7}$$

where $K = A + \beta(B^3/A^2)$. Hydrostatic pressure is measured by

$$p = \frac{1}{3}\sigma_{ii} = \frac{1}{3}I. \tag{4.8}$$

Strain rate is measured by the distortion strain rate,

$$\frac{\dot{\gamma}}{r\sqrt{2}} = \dot{\lambda}, \quad r = \left(\frac{\partial g}{\partial \sigma'_{ij}}\frac{\partial g}{\partial \sigma'_{ij}}\right)^{1/2}, \tag{4.9}$$

and the volumetric strain rate,

$$\frac{\dot{v}}{v} = D_{ii}. \tag{4.10}$$

In this and following sections it is assumed that the elastic part of the deformation rate is negligible. For simplicity in notation, the superscript p on the plastic part of the deformation rate is deleted.

The state of stress is uniquely defined by the scalars Kq and ρ. The coefficient K includes the effect of the intermediate principal stress, and is plotted in Fig. 3 for various values of β. The necessity of including J_3 in the measure of distortional stress is apparent from the curve for $\beta = 0$, which is symmetric with respect to $b = 0.5$. However each b in the range $0 < b < 1$ defines a unique state of stress. Consequently each b should have a unique representation for distortional stress (i.e. a unique K), and $J^{1/2}$ alone is not sufficient.

The scalar measures of stress and strain can now be used to calculate the rate of plastic work. The rate of plastic work can then be compared with an approximation for the rate of energy dissipation due to friction to obtain an expression relating $(\partial F/\partial I)$ and $(\partial G/\partial I)$.

Consider first the rate of distortional plastic work per unit current volume,

$$\frac{\rho}{\rho_o}\dot{\xi} = \sigma'_{ij}D_{ij} = \sigma'_{ij}D'_{ij} = \frac{1}{r\sqrt{2}}\dot{\gamma}\sigma'_{ij}\frac{\partial g}{\partial \sigma'_{ij}} = \frac{K}{r\sqrt{2}}q\dot{\gamma}. \tag{4.11}$$

Use $c(\eta) = \beta\eta$ to obtain

$$r = \left(\frac{1}{2} + \beta\eta + \beta^2(2/3 - 4\eta^2)\right)^{1/2}. \tag{4.12}$$

This is plotted in Fig. 4 as a function of b for various values of β. The total rate of plastic work per unit current volume is

$$\dot{w}_p = \sigma_{ij}D_{ij} = \left(\sigma'_{ij} + \frac{1}{3}\sigma_{kk}\delta_{ij}\right)D_{ij} = \frac{K}{r\sqrt{2}}q\dot{\gamma} + p\frac{\dot{v}}{v}. \tag{4.13}$$

From the yield condition,

$$f \equiv K\tau - F, \tag{4.14}$$

it follows that

$$\frac{\mathrm{d}\tau}{\mathrm{d}p} = \frac{1}{K}\frac{\partial F}{\partial p} \tag{4.15}$$

measures the change in resistance to flow per unit change in pressure. The quantity $(1/K)$ introduces the effect of stress triaxiality, and $(\partial F/\partial p)$ is a material property which is related to the coefficient of sliding friction. If $(\partial F/\partial p)$ is constant then the frictional shear stress is

$$\tau_f = \frac{1}{K}\frac{\partial F}{\partial p}p. \tag{4.16}$$

However granular materials consist of discrete particles which transmit normal and shear forces across the contact areas of each particle. Within a unit volume there will be, say, N points of active slip which give rise to the total *effective* plastic shear strain rate,

$$\dot{\gamma} = \sum_{i=1}^{N} \dot{\gamma}^i, \tag{4.17}$$

where $\dot{\gamma}^i$ is the effective strain rate contributed by the ith slip system. Let τ_f^i be the resistive force at the ith slip. Then the rate of energy loss is

$$\dot{w}_f = \sum_{i=1}^{N} \tau_f^i \dot{\gamma}^i. \tag{4.18}$$

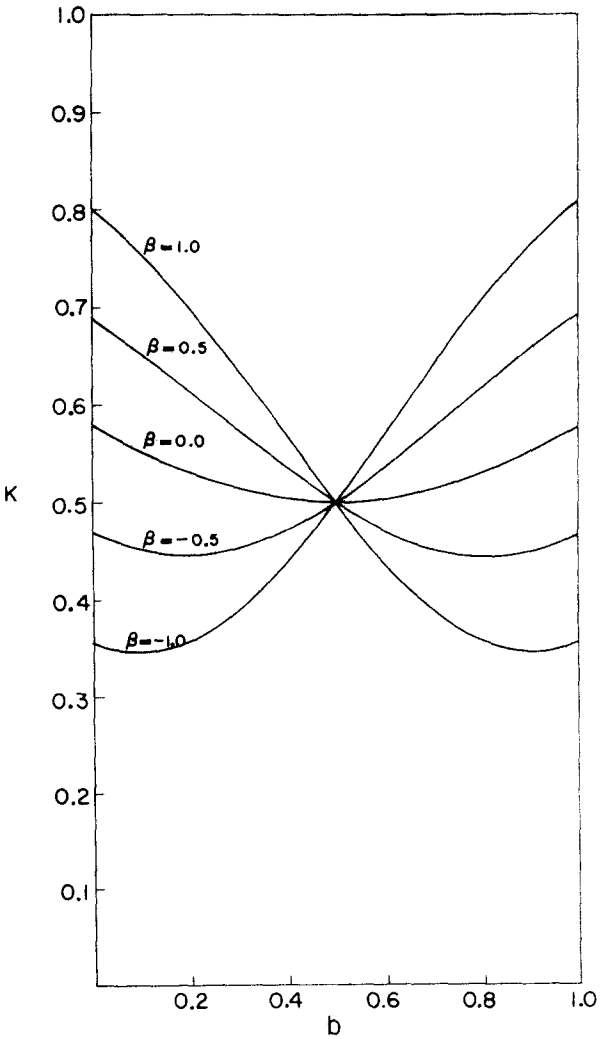

Fig. 3. Variation of the parameter K with b, for indicated values of β.

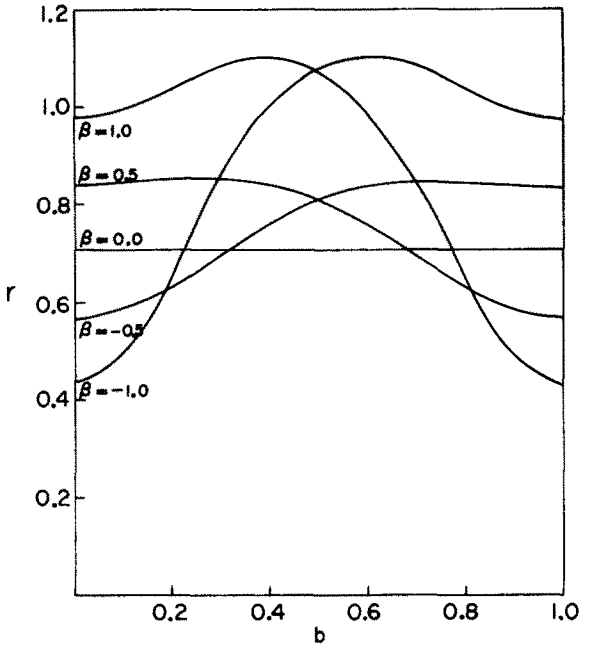

Fig. 4. Variation of the parameter r with b, for indicated values of β.

If $(1/K)(\partial F/\partial p)p$ is interpreted as the average frictional resistance, then (4.18) yields

$$\dot{w}_f \simeq \frac{1}{K}\frac{\partial F}{\partial p}p\sum_{i=1}^{N}\dot{\gamma}^i = \frac{1}{K}\frac{\partial F}{\partial p}p\dot{\gamma}. \tag{4.19}$$

For an ideal granular material consisting of rigid particles, the rate of friction loss must equal the rate of plastic work. Equating (4.19) and (4.13) and employing (3.5) we find

$$3\frac{\partial G}{\partial I} = \frac{\partial G}{\partial p} = \frac{r\sqrt{2}}{K}\frac{\partial F}{\partial p} - K\frac{q}{p}. \tag{4.20}$$

This result shows that the dilatancy factor is a quantity distinct from the friction factor and demonstrates the need for a non-associated flow rule for granular materials. Equation (4.20) relates $(\partial G/\partial p)$ and $(\partial F/\partial p)$ for the special case of an ideal granular material. If we set $M = (r\sqrt{2}/K^2)(\partial F/\partial p)$, it then follows from the definition of $(\partial G/\partial p)$ that, $M < (q/p)$ defines dilation, $M > (q/p)$ defines densification, and $M = (q/p)$ defines the critical state. These are the same conditions, shown in Fig. 5, proposed by Schofield and Wroth[28] in their critical state soil mechanics except that in the present case the coefficient M depends on the intermediate principal stress via the parameter b. It should be noted that although eqn (4.20) is based on a simple approximation for the rate of frictional loss, the parameter β can be adjusted so that the result can have a wide range of applicability.

Finally substitute for $\dot{\lambda}$ in (2.7), multiply by σ'_{ij}, and equate with (4.11) to obtain

$$(1+c)\frac{dJ^{1/2}}{d\gamma} + J^{1/2}\frac{dc}{d\gamma} - \frac{\partial F}{\partial I}\frac{dI}{d\gamma} = \frac{H}{r\sqrt{2}} = \frac{1}{r\sqrt{2}}\frac{\rho_0}{\rho}\left[3\frac{\partial G}{\partial I}\frac{\partial F}{\partial \Delta} + J^{1/2}(1+c)\frac{\partial F}{\partial \xi}\right]. \tag{4.21}$$

Substituting for c, using (4.11) and (4.20), and rearranging we arrive at

$$\frac{dJ^{1/2}}{d\gamma} + \beta\frac{d}{d\gamma}\left(\frac{J_3}{J}\right) + \frac{J_3}{J}\frac{d\beta}{d\gamma} - \frac{\partial F}{\partial p}\frac{dp}{d\gamma} = \frac{1}{r\sqrt{2}}(1-\Delta)\frac{\partial F}{\partial \Delta}\left(\frac{r\sqrt{2}}{K}\frac{\partial F}{\partial p} - K\frac{q}{p}\right) + \frac{\partial F}{\partial \gamma}. \tag{4.22}$$

Equations (4.22) and (3.6) are two coupled ordinary differential equations relating q, p and Δ as

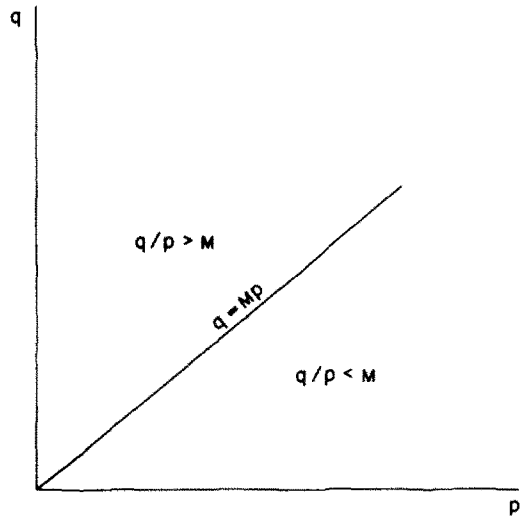

Fig. 5. The critical curve in the q,p-plane for a cohesionless granular material.

functions of γ. These two equations along with the initial conditions $q = 0$ and $\Delta = 0$ at $\gamma = 0$ describe the behavior of an ideal cohesionless granular material under a triaxial state of stress, *for monotone loading.*

To compare these equations with experiments we choose the results of Lade and Duncan [4] since they not only present stress and volume strain data, but also show a complete strain history. It is now necessary to modify our equations to duplicate the test procedures of Lade and Duncan.

Their tests were performed for a particular b by initially consolidating the sample under a hydrostatic pressure. The minor principal stress, σ_3, is held constant while the sample is sheared to failure by increasing σ_2 and σ_1 in such a manner that b remains constant. Thus in (4.22), $(db/d\gamma) = (d\beta/d\gamma) = 0$. For this loading procedure the hydrostatic pressure is

$$p = \frac{1}{3}(b+1)q + \sigma_3. \tag{4.23}$$

Thus $(dp/d\gamma) = (1/3)(b+1)(dq/d\gamma)$ and eqn (4.22) becomes

$$\left[K - \frac{1}{3}(b+1)\frac{\partial F}{\partial p}\right]\frac{dq}{d\gamma} = \frac{1}{r\sqrt{2}}(1-\Delta)\frac{\partial F}{\partial \Delta}\left(\frac{r\sqrt{2}}{K}\frac{\partial F}{\partial p} - K\frac{q}{p}\right) + \frac{\partial F}{\partial \gamma}. \tag{4.24}$$

All results of Lade and Duncan are presented as functions of ϵ_{11}. Thus take ϵ_{11} as the "time" parameter, and apply the chain rule to (4.24) and (3.6) to obtain

$$\left[K - \frac{1}{3}(b+1)\frac{\partial F}{\partial p}\right]\frac{dq}{d\epsilon_{11}}\frac{d\epsilon_{11}}{d\gamma} = \frac{1}{r\sqrt{2}}(1-\Delta)\frac{\partial F}{\partial \Delta}\left(\frac{r\sqrt{2}}{K}\frac{\partial F}{\partial p} - K\frac{q}{p}\right) + \frac{\partial F}{\partial \epsilon_{11}}\frac{d\epsilon_{11}}{d\gamma}, \tag{4.25}$$

$$\frac{d\Delta}{d\epsilon_{11}}\frac{d\epsilon_{11}}{d\gamma} = \frac{1}{r\sqrt{2}}(1-\Delta)\left(\frac{r\sqrt{2}}{K}\frac{\partial F}{\partial p} - K\frac{q}{p}\right).$$

The quantity $(d\epsilon_{11}/d\gamma)$ is easily calculated from (4.11),

$$\frac{d\epsilon_{11}}{d\gamma} = \frac{3K}{r\sqrt{(2)}D}, \tag{4.26}$$

where

$$D = (2-b) + (2b-1)\frac{d\epsilon_{22}}{d\epsilon_{11}} - (b+1)\frac{d\epsilon_{33}}{d\epsilon_{11}}. \tag{4.27}$$

Utilizing eqn (2.7), we find

$$\frac{d\epsilon_{22}}{d\epsilon_{11}} = \frac{D_{22}}{D_{11}} = \frac{\frac{\beta}{3A^2}(2b-1)^2 + \left(\frac{1}{2A} - \beta\frac{B^3}{A^4}\right)(2b-1) - 2\beta + \frac{\partial G}{\partial p}}{\frac{\beta}{3A^2}(2-b)^2 + \left(\frac{1}{2A} - \beta\frac{B^3}{A^4}\right)(2-b) - 2\beta + \frac{\partial G}{\partial p}},$$

$$\frac{d\epsilon_{33}}{d\epsilon_{11}} = \frac{D_{33}}{D_{11}} = \frac{\frac{\beta}{3A^2}(b+1)^2 - \left(\frac{1}{2A} - \beta\frac{B^3}{A^4}\right)(b+1) - 2\beta + \frac{\partial G}{\partial p}}{\frac{\beta}{3A^2}(2-b)^2 + \left(\frac{1}{2A} - \beta\frac{B^3}{A^4}\right)(2-b) - 2\beta + \frac{\partial G}{\partial p}}. \tag{4.28}$$

These equations show that for a given b, $(d\epsilon_{22}/d\epsilon_{11})$ and $(d\epsilon_{33}/d\epsilon_{11})$ are functions of β and $(\partial G/\partial p)$. For the axially symmetric cases (i.e. $b = 0$, $b = 1$) two strains are always equal so that only one of the above equations is independent. Thus for $b = 0$ and $b = 1$, the theory of Nemat-Nasser and Shokooh[8] is sufficient to predict the strains with $\beta = 0$. However for $0 < b < 1$, $(\partial G/\partial p)$ does not in general satisfy the equations in (4.28) simultaneously. An additional parameter is required and hence $\beta \neq 0$ for $0 < b < 1$.

The constitutive parameters $(\partial F/\partial \Delta)$ and $(\partial F/\partial \gamma)$ measure the relative strengths of the density-hardening (or -softening) and distortional hardening terms. Assume $(\partial F/\partial \Delta) = ap$ since initial density-hardening depends on the initial consolidation pressure, and set $(\partial F/\partial \gamma) = (\partial F/\partial \epsilon_{11})(\partial \epsilon_{11}/\partial \gamma) = (\partial \epsilon_{11}/\partial \gamma)\hat{h}e^{-\hat{\rho}\epsilon_{11}}$ since distortional hardening is a monotonically decreasing function of strain. The quantities a and $\hat{h}$ are assumed to be constants which depend on b, and $\hat{\rho}$ is arbitrarily chosen as $\hat{\rho} = 50$. The friction factor, $(\partial F/\partial p)$, is also assumed to be a different constant for each b.

The true triaxial tests of Lade and Duncan[4] were performed on loose and dense samples of Monterey No. 0 sand with initial void ratios of $e_o = 0.78$ and $e_o = 0.57$ respectively. Equation (4.25) is normalized with respect to σ_3, and both coupled differential equations (4.25) depend on the four parameters a, $\hat{h}$, $(\partial F/\partial p)$ and β. *The values of these parameters are fixed by comparison with the observed stresses and strains at the peak strengths of the samples.* However, due to the basic differences in the behavior of loose and dense samples at the peak strength, different assumptions should be made concerning the actual values of the parameters.

For dense sands it may be assumed that the sample is stable until the peak strength is attained. As a consequence the strain measurements should be reasonably accurate. Measurement of $(d\epsilon_{22}/d\epsilon_{11})$ and $(d\epsilon_{33}/d\epsilon_{11})$ at the peak strength along with (4.28) yields two simultaneous equations for β and $(\partial G/\partial p)$ at peak strength. Once β is determined, (4.20) is utilized to calculate $(\partial F/\partial p)$. The quantities a and $\hat{h}$ are determined by matching the calculated peak strength with the observed strength and requiring $(d\bar{q}/d\epsilon_{11}) = 0$ at the peak strength. Here $\bar{q}$ denotes the normalized shear stress, q/σ_3.

Loose sand on the other hand is *inherently unstable* at stresses *below* the final strength. Because the distortional hardening is negligible for loose sands, the critical state is approached (i.e. $(\partial G/\partial p) \to 0$) as the peak strength is approached, and the material behaves more like a frictional fluid than a solid which can support shear stresses. For this reason, data for truly loose sand are not readily obtainable, and, because of the inherently unstable response, an initially loose sand may undergo large densification upon loading which then renders the sample dense. In fact the observed volume strains for the loose samples in experiments by Lade and Duncan[4] are similar to those of their dense samples (i.e. initial densification followed by dilatancy, instead of monotonic densification). This indicates that the assumption of loose-sand behavior may not be appropriate in comparing the theoretical predictions with these experimental results. Notwithstanding this, we have made such a comparison in the following manner. We assume that $(\partial G/\partial p) = 0$ at the observed peak strength and measure $(d\epsilon_{22}/d\epsilon_{11})$ and $(d\epsilon_{33}/d\epsilon_{11})$ at the peak. These measurements along with eqns (4.28) provide two independent equations for β. We choose β to be the average value of the two solutions. We assume $\hat{h} = 0$ and choose a by matching the observed and calculated peak strengths. Note that this assumption then precludes dilatancy in the theoretical results. Again $(\partial F/\partial p)$ is calculated from (4.20).

Once all parameters are determined, eqns (4.25) can be integrated simultaneously for $\bar{q}$ and Δ. After the stresses are calculated the strains are found by integration of (4.28). All calculated quantities for both loose and dense sand are shown in Figs. 6–17 along with the data of Lade and Duncan[4].

The calculated stresses show good agreement with the observed stresses at the peak strength for both the loose and dense samples. However the initial slopes of all calculated stress, strain-curves underestimate the initial strengths of the samples. This is a result of the assumption that a (i.e. $(1/p)(\partial F/\partial\Delta)$ is constant throughout the test. Since both loose and dense samples of sand are observed to initially compact, a should initially increase and be a function of Δ. This would result in a higher initial slope for the stress, strain-curves. The calculated strains also show good agreement with the observed strains at peak strength.

Since all parameters are chosen from data for stresses and strains at the peak strength, the calculated void ratios are a direct result of the theory. As discussed above, comparison with the volume data for loose sand is not considered appropriate due to material instability and the fact that $\hat{h} = 0$ is assumed. Consequently the poor agreement between the calculated and observed void ratios of loose sand is expected; the calculated void ratios do show the behavior typical of loose sand, i.e. no dilatancy. The calculated void ratios for dense sand do show good correlation with the experimental data and lend support to the theory. Note further that *the experimental results for the loose sand can be matched much better than shown, if the loose sand is treated as if it were a dense sand*, i.e. by assuming that the distortional hardening is not zero ($\hat{h} \neq 0$).

The use of strain component as the independent parameter can lead to confusion in the interpretation of the results when considering a series of tests covering the whole range of $0 \leq b \leq 1$. For example, ϵ_{11} represents the axial strain for $b = 0$ in Fig. 6 and the lateral strain for $b = 1$ in Fig. 10. A more natural choice for the independent parameter would be γ. This choice yields a simple estimation for the plastic distortional work by calculating the area under the q, γ – curve. In Fig. 18, $\bar{q}$ is plotted as a function of γ using the same parameters as those in Figs. 6–10.

5. DISCUSSION OF RESULTS

The preceding results are obtained by introducing the quantities r and K into the constitutive relations. The roles of r and K are best interpreted by considering the conventional triaxial tests as limiting cases. The conventional triaxial tests define an axially symmetric state of stress, and yield a simple expression for the plastic distortional work in terms of the principal stress and strain differences. For the axially symmetric states of stress, Nemat-Nasser and Shokooh[8] show that if the distortional stress is $q = \sigma_1 - \sigma_3$ and the distortional strain rate is $\dot{\epsilon} = (2/3)(\dot{\epsilon}_{11} - \dot{\epsilon}_{33}) = (1/\sqrt{3})\dot{\gamma}$, then the rate of distortional plastic work per unit current volume is $(\rho/\rho_o)\dot{\xi} = q\ \dot{\epsilon} = (1/\sqrt{3})q\dot{\gamma}$. However in a true triaxial state of stress, there are three principal stress and strain differences, and it is not clear what the representative measure of distortional stress and strain should be. By introducing $c(\eta) = \beta(J_3/J^{3/2})$ into the plastic potential, it has been shown in (4.11) that $(\rho/\rho_o)\dot{\xi} = (K/r\sqrt{2})q\dot{\gamma}$. Here $K\,q$ is the distortional stress and $(\dot{\gamma}/r\sqrt{2})$ is the conjugate distortional strain rate. When $\beta = 0$, $K = (1/\sqrt{3})$ and $r = (1/\sqrt{2})$ so that $(K/r\sqrt{2})q\dot{\gamma}$ reduces to the expression of plastic work for the axially symmetric state of stress. Here the parameters K and r can be interpreted as "correction" factors which adjust the measures of distortional stress, q, and the distortional strain, γ, to include the effect of the intermediate principal stress. In this sense r and K generalize the axially symmetric state of stress to a triaxial state of stress.

The quantities K are r are functions of β. The three quantities r, K, and β are shown in Figs. 19–21 as functions of b. A characteristic of these graphs is the discontinuity at $b = 0$. At first it may seem unreasonable that these discontinuities should exist, but they can be understood by the following consideration. The connection of β and $(\partial G/\partial p)$ with the correct predictions of strain has already been discussed. For the dense sand the dilatancy factor at peak strength, denoted by $(\partial G/\partial p)_{cr}$ is shown in Fig. 22. This figure shows $(\partial G/\partial p)_{cr}$ to be constant and indicates that there may be a constant critical dilatancy factor associated with the peak strength of a dense granular material. At peak strengths it is observed that $(d\epsilon_{22}/d\epsilon_{11})$ and $(d\epsilon_{33}/d\epsilon_{11})$ change monotonically as functions of b (see Figs. 11 and 12). Since $\partial G/\partial p)_{cr}$ is constant and β is fixed for each particular b, it follows that β should be monotonic. However,

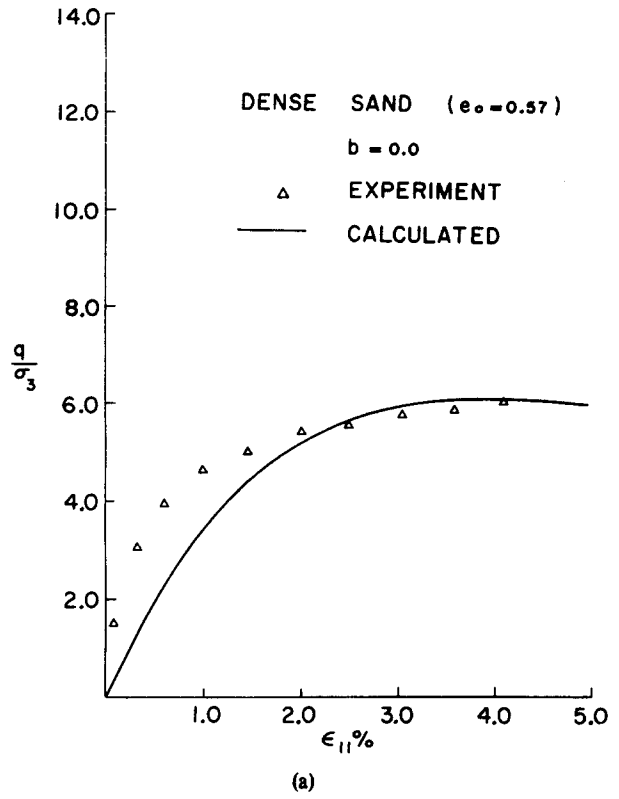

Fig. 6. Normalized shear stress, q/σ_3, and void ratio, e, as functions of ϵ_{11} in true triaxial test of Monterey No. 0 sand; Experimental data from Lade and Duncan[4].

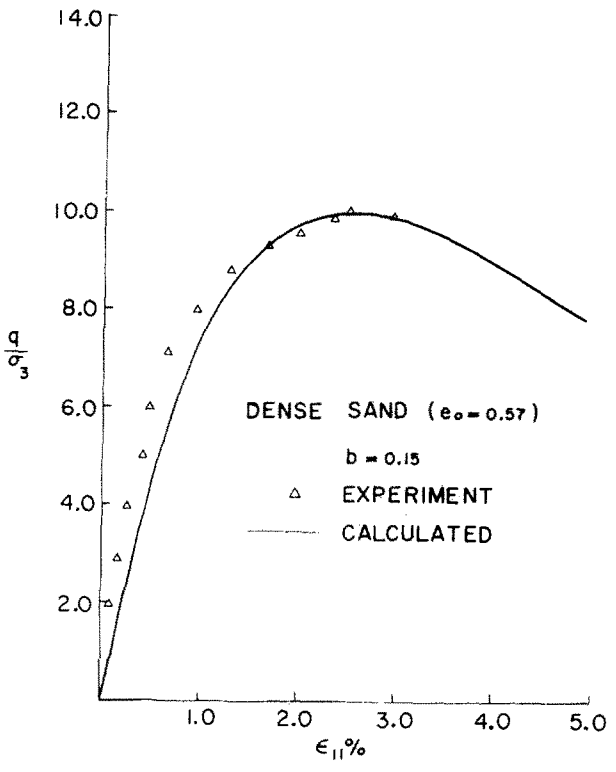

(a)

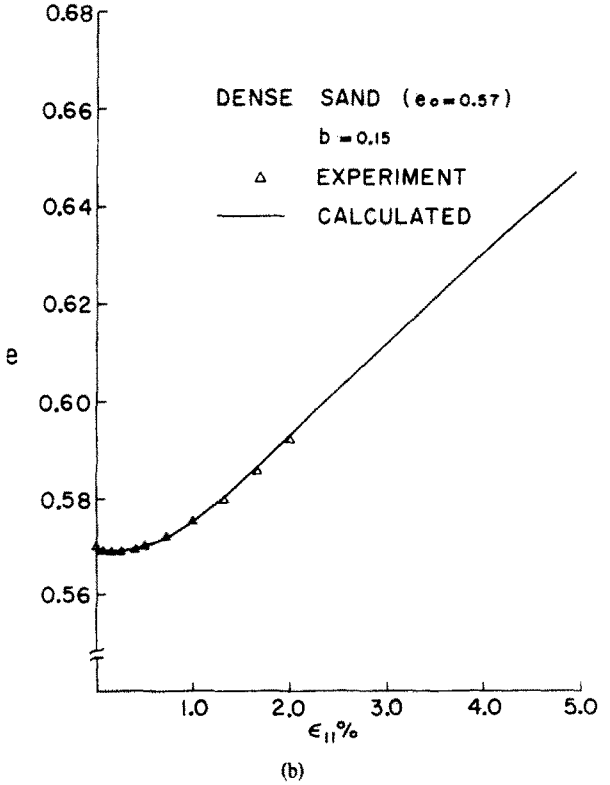

(b)

Fig. 7. Normalized shear stress, q/σ_3, and void ratio, e, as functions of ϵ_{11} in true triaxial test of Monterey No. 0 sand; Experimental data from Lade and Duncan[4].

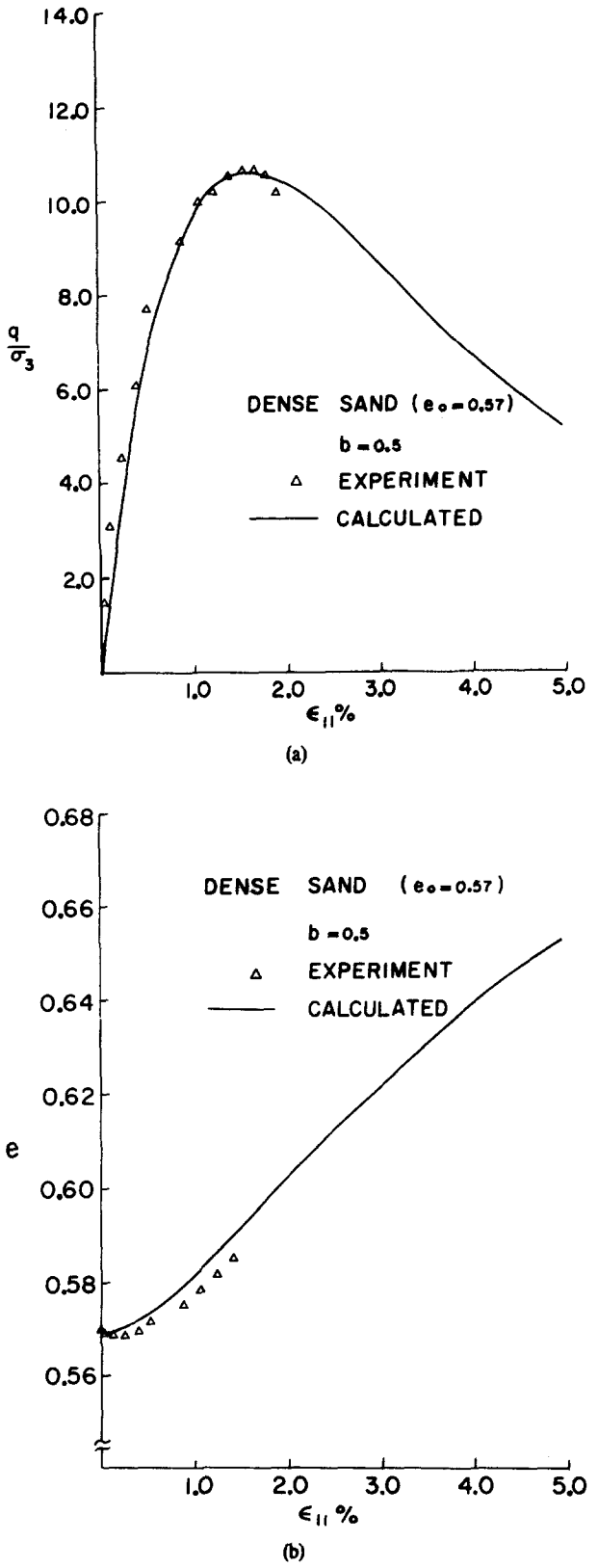

Fig. 8. Normalized shear stress, q/σ_3, and void ratio, e, as functions of ϵ_{11} in true triaxial test of Monterey No. 0 sand; Experimental data from Lade and Duncan[4].

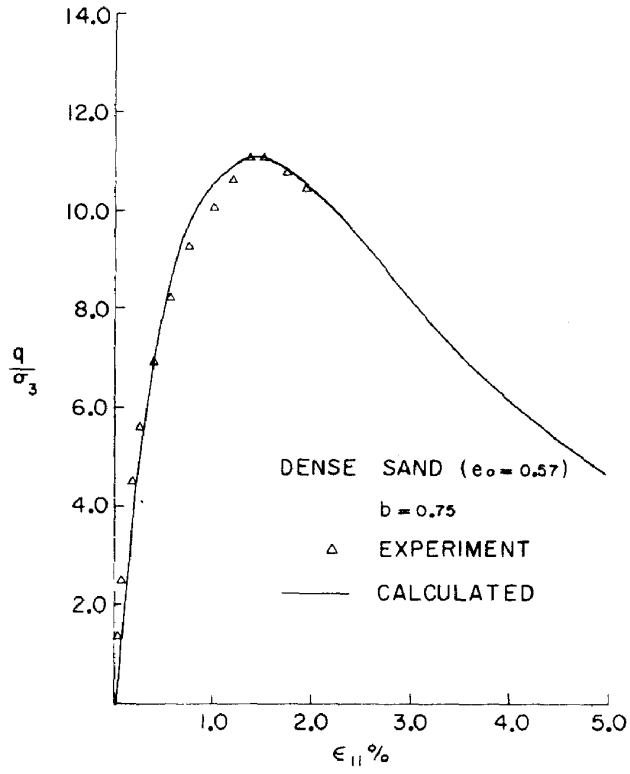

(a)

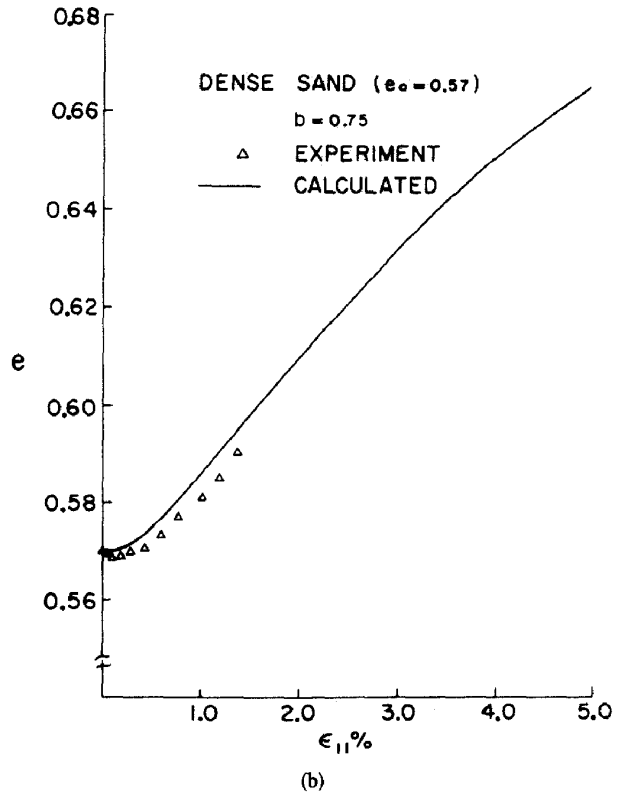

(b)

Fig. 9. Normalized shear stress, q/σ_3, and void ratio, e, as functions of ϵ_{11} in true triaxial test of Monterey No. 0 sand; Experimental data from Lade and Duncan[4].

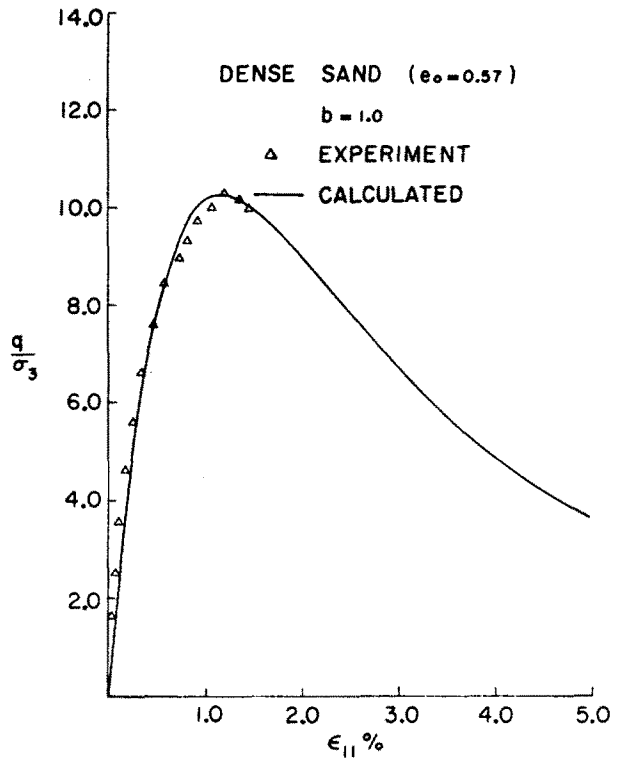

(a)

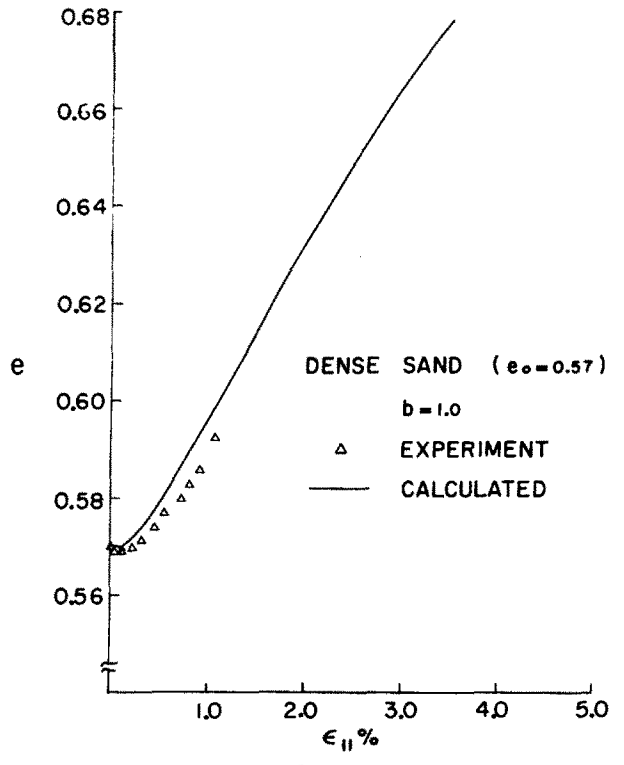

(b)

Fig. 10. Normalized shear stress, q/σ_3, and void ratio, e, as functions of ϵ_{11} in true triaxial test of Monterey No. 0 sand; Experimental data from Lade and Duncan[4].

we have already chosen $\beta = 0$ for $b = 0$ and $b = 1$. Hence β should be discontinuous at an endpoint of the interval $0 \leq b \leq 1$. Similarly, any b in the interval $0 < b < 1$ defines a unique state of stress and it follows that K should be monotonic on that interval. On the other hand $K = (1/\sqrt{3})$ has already been chosen for both $b = 0$ and $b = 1$. Hence K should also be discontinuous at an endpoint of the interval $0 \leq b \leq 1$. The quantity r is defined as the magnitude of $(\partial g/\partial \sigma'_{ij})$ and from eqn (4.12), it is seen that r is a function of β. Since β is discontinuous we conclude that r should also be discontinuous. The discontinuities can occur at either $b = 0$ (i.e. $\sigma_2 = \sigma_3$) or at $b = 1$ (i.e. $\sigma_2 = \sigma_1$). In the present case they appear at $b = 0$ due to our definition of b. Finally we note from Figs. 19, 20, and 21, that the quantities r, K and β depend on the state of stress and are independent of the initial void ratio.

The quantity $(\partial F/\partial p)$ is calculated from (4.20). Figure 23 shows that $(\partial F/\partial p)$ depends on the initial void ratio and is constant on the interval $0 < b \leq 1$. Again a discontinuity is observed at $b = 0$ and is justified by considering the axially symmetric states of stress. For the program of loading in the series of tests, the hydrostatic pressure is given by $p = (1/3)(b + 1)q + \sigma_3$ which implies $(dq/dp) = 3/(b + 1)$. Thus the unit change in shear per unit change in pressure for $b = 0$ is twice as large as for $b = 1$. In (4.15) we define the change in resistance to flow per unit change in pressure as $(1/K)(\partial F/\partial p)$. Since $b = 0$ and $b = 1$ yield the same K, the constitutive parameter $(\partial F/\partial p)$ must be changed to allow for the different load paths followed in each test. In fact for the tests on dense sand the calculated (on the basis of experimental results) value of $(\partial F/\partial p)$ for $b = 0$ is exactly twice as large as that for $b = 1$.

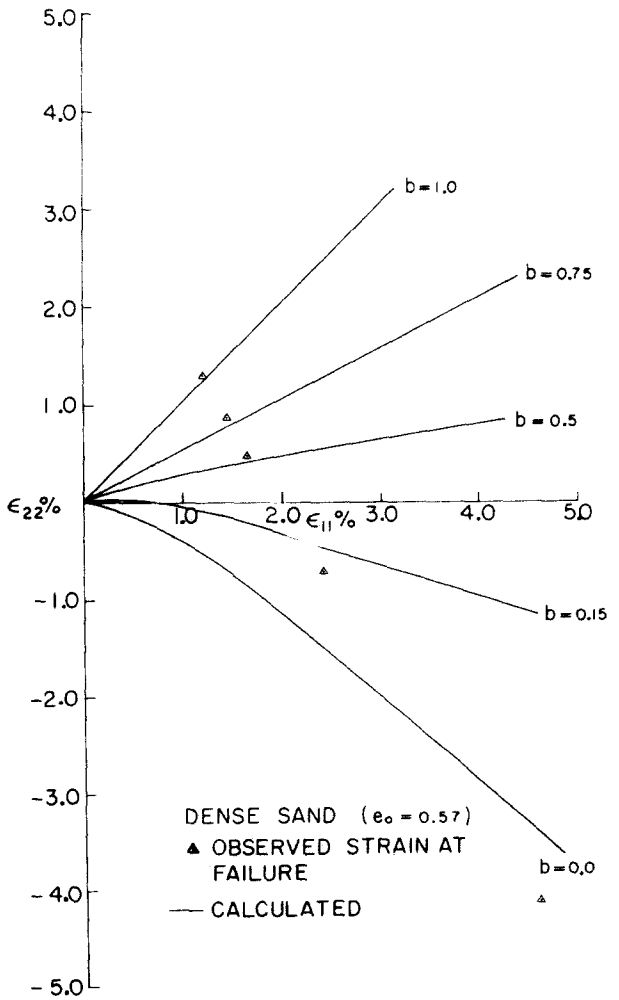

Fig. 11. ϵ_{22} as a function of ϵ_{11} for indicated values of b in true triaxial tests of Monterey No. 0 sand; Experimental data from Lade and Duncan[4].

Several quantities when plotted as functions of b are found to be continuous on the interval $0 \leq b \leq 1$. These quantities have clear physical interpretations in contrast to the discontinuous quantities which appear as a result of definition. Figure 24 shows the variation of (K/r) with b. For a given q and strain rate, $\dot{\gamma}$, this quantity measures the rate of plastic distortional work (see eqn 4.11). This figure shows the rate of plastic work to be a minimum for the axially symmetric states of stress and a maximum near the plane strain value of b. The continuous quantity, $(1/K)(\partial F/\partial p)$, is shown in Fig. 25 and is a measure at the microscopic level, of the materials' resistance to plastic flow (see eqn 4.15). The critical line, $(q/p) = (r\sqrt{2}/K^2)(\partial F/\partial p)$, is found to be linear for both loose and dense samples and is illustrated in Fig. 26. The quantities $(1/K)(\partial F/\partial p)$ and $(r\sqrt{2}/K^2)(\partial F/\partial p)$ depend on $(\partial F/\partial p)$ and as a result depend on the initial void ratio, while (K/r) just depends on the state of stress.

5.1 *Some basic observations*

It is impossible to make any conclusions regarding the behavior of granular materials in general on the basis of applying the theory to one set of experimental data. However the results presented here suggest a simple method of predicting the shear strength of granular materials. The method depends on the general validity of three conditions observed in Figs. 22, 23 and 26. These conditions are:

(1) There exists a critical value of the dilatancy factor at peak strength of the sample. For loose sands, $(\partial G/\partial p)_{cr} = 0$, and for dense sands $(\partial G/\partial p)_{cr} < 0$.

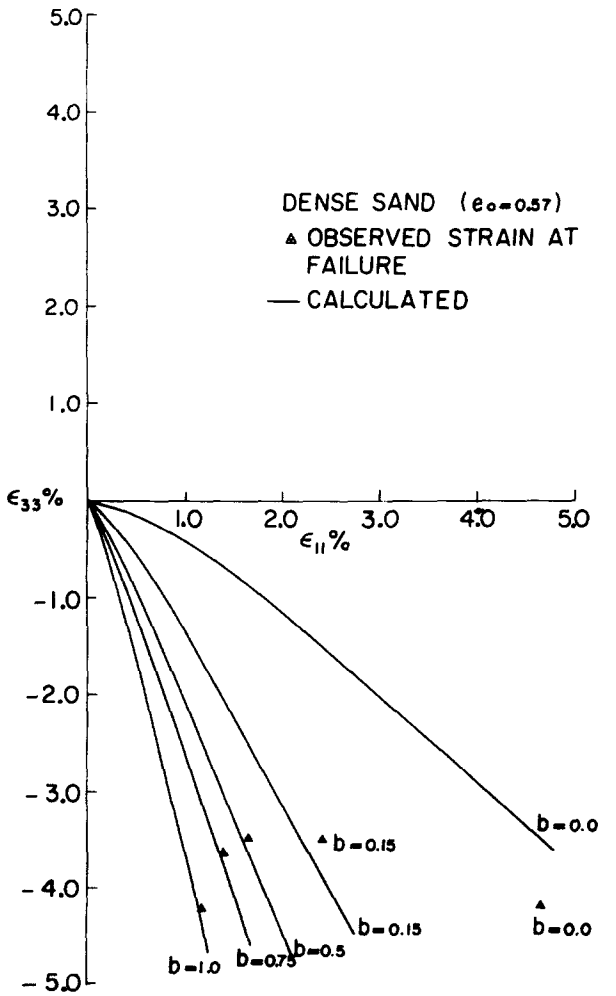

Fig. 12. ϵ_{33} as a function of ϵ_{11} for indicated values of b in true triaxial tests of Monterey No. 0 sand; Experimental data from Lade and Duncan[4].

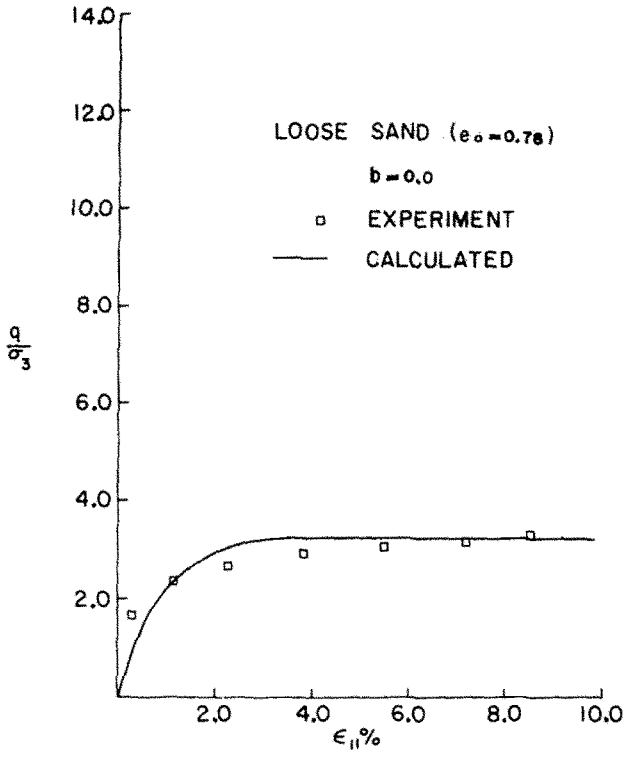

(a)

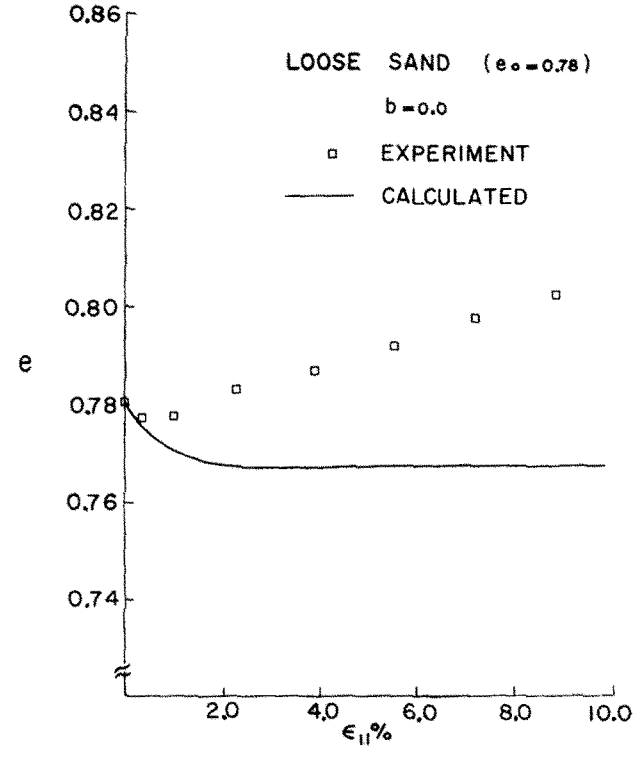

(b)

Fig. 13. Normalized shear stress, q/σ_3, and void ratio, e, as functions of ϵ_{11} in true triaxial test of Monterey No. 0 sand; Experimental data from Lade and Duncan[4].

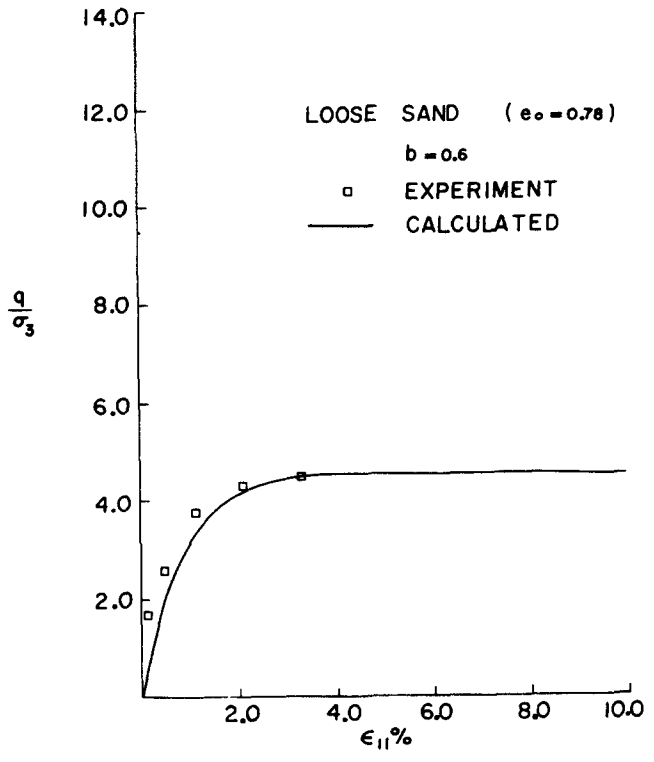

(a)

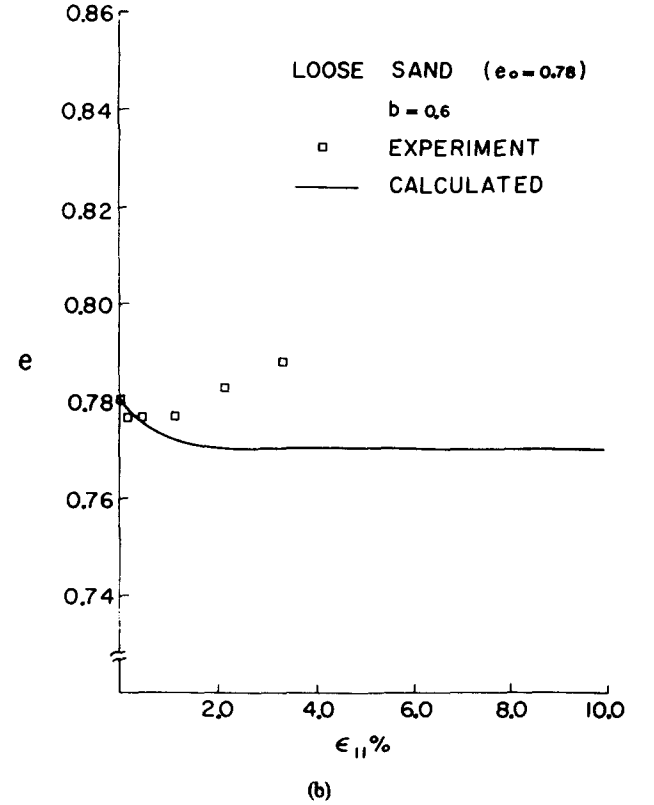

(b)

Fig. 14. Normalized shear stress, q/σ_3, and void ratio, e, as functions of ϵ_{11} in true triaxial test of Monterey No. 0 sand; Experimental data from Lade and Duncan[4].

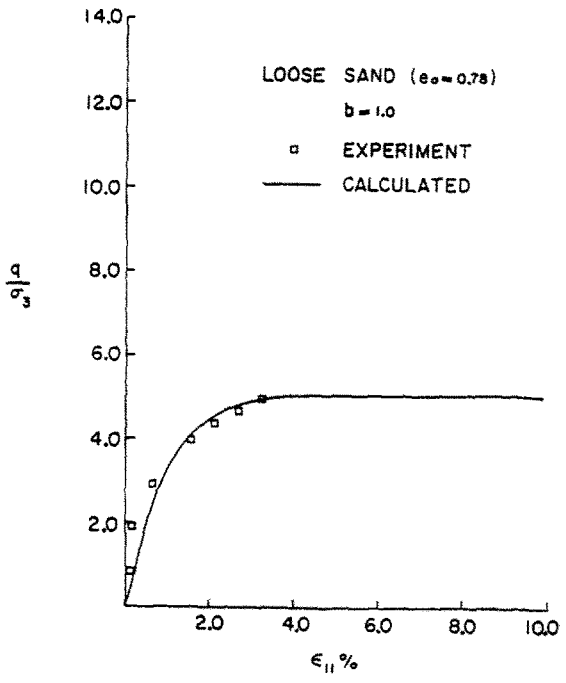

(a)

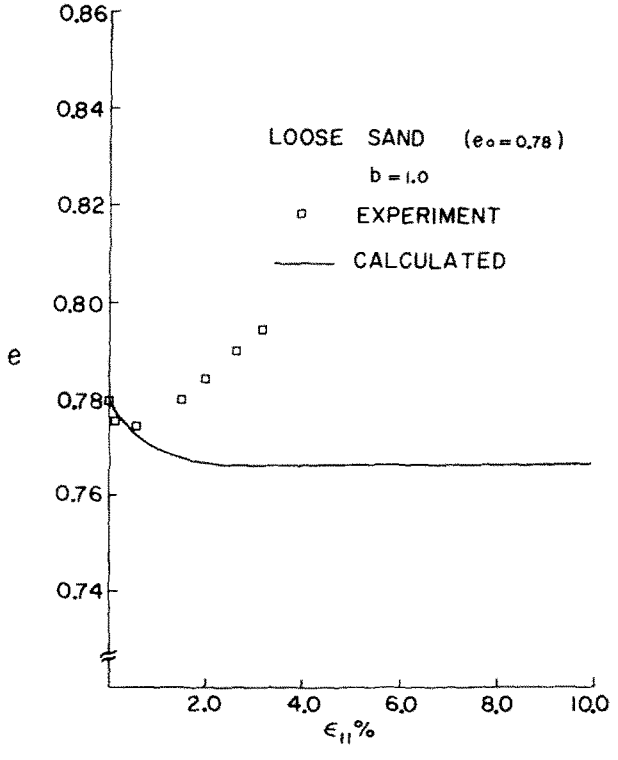

(b)

Fig. 15. Normalized shear stress, q/σ_3, and void ratio, e, as functions of ϵ_{11} in true triaxial test of Monterey No. 0 sand; Experimental data from Lade and Duncan[4].

(2) The quantity $(\partial F/\partial p)$ (the overall friction coefficient) is constant on the interval $0 < b \leq 1$.

(3) The quantity $(r\sqrt{2}/K^2)(\partial F/\partial p)$ is linear on the interval $0 \leq b \leq 1$. If these conditions are in general valid, then the shear strength of a cohesionless granular material can be predicted for any b from results obtained on tests for $b = 0$ and $b = 1$, i.e. from the *conventional* triaxial tests in compression and in tension.

Assuming that these conditions are in general true, the tests for $b = 0$ and $b = 1$ can be performed to establish the linear dependence of $(r\sqrt{2}/K^2)(\partial F/\partial p)$ on b. The test for $b = 1$ also determines $(\partial F/\partial p)$ and $(\partial G/\partial p)_{cr}$. Since $(r\sqrt{2}/K^2)(\partial F/\partial p)$ is known for any b, the expressions for r and K along with the calculated value of $(\partial F/\partial p)$ are substituted into $(r\sqrt{2}/K^2)(\partial F/\partial p)$ to yield a fourth degree polynomial in β. The proper solution of this polynomial is the value of β which yields positive and real values of r and K. Once β is determined, (4.20) is used to calculate the peak strength. It should be emphasized that this method depends on the validity of conditions (1)–(3), and extensive tests need to be performed over a wide range of materials and void ratios to test their general validity.

Finally the quantities a and $\hat{h}$ are normalized with respect to the values of a and $\hat{h}$ calculated at $b = 0$ and are shown in Figs. 27 and 28. The quantity a is observed to have a peak value for both loose and dense samples while $\hat{h}$ increases monotonically for dense sands. It should be noted that a and $\hat{h}$ are in general functions of strain and these figures represent at best the variation of $(\partial F/\partial \Delta)$ and $(\partial F/\partial \gamma)$ at peak strength.

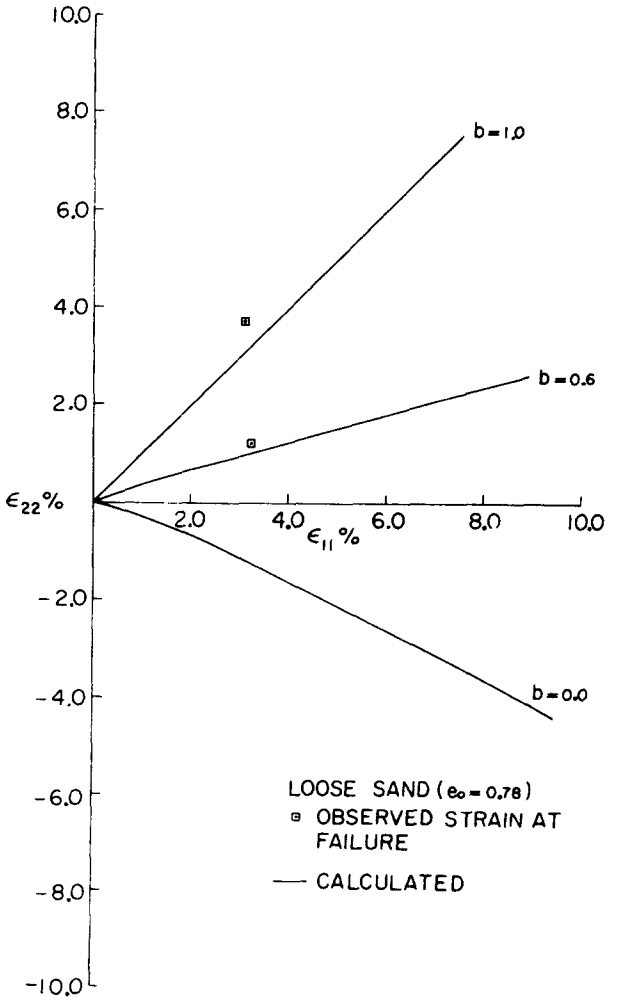

Fig. 16. ϵ_{22} as a function of ϵ_{11} for indicated values of b in true triaxial tests of Monterey No. 0 sand; Experimental data from Lade and Duncan[4].

5.2 *Additional comments*

To describe a physical phenomenon, such as the deformation of a granular mass, it is relatively easy to empirically establish equations with enough parameters which can fit any set of data. Then the mathematical description of an observed phenomenon reduces to a process of curve fitting. An indication that a theory is based on sound physical principles, rather than empirical observation, is its dependence on a few parameters with clear physical interpretations, and with enough flexibility to cover a wide range of applications. The functions F and G in the present theory provide this flexibility, and lead to parameters with physical interpretations. In Section 4 we have shown that only four parameters are needed to adequately describe all quantities of interest in the true triaxial test. We will now obtain solutions to (4.25), independent of any *quantitative* comparison with experiments, and demonstrate that eqn (4.25) contains *qualitatively* the features of a true triaxial test. To show this, solutions are obtained based on the following simplifying assumptions:†

(1) $(\partial F/\partial p)$ is constant for all b.

(2) $(\partial F/\partial \epsilon_{11}) = \hat{h}e^{-\hat{\rho}\epsilon_{11}}$. The quantities $\hat{h}$ and $\hat{\rho}$ are positive and constant for all b.

(3) $(1-\Delta) \simeq 1$. This assumption uncouples the differential equation and is reasonable for small strain.

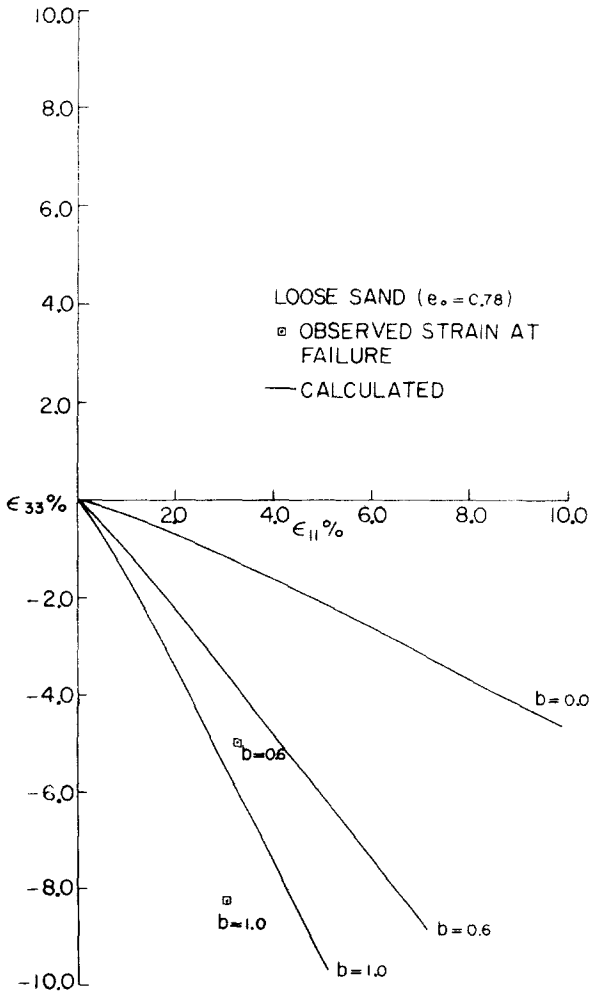

Fig. 17. ϵ_{33} as a function of ϵ_{11} for indicated values of b in true triaxial tests of Monterey No. 0 sand; Experimental data from Lade and Duncan[4].

†Note that these assumptions are introduced here to simplify the mathematics. They have *not* been used in the preceding sections where comparison with actual experimental results has been presented.

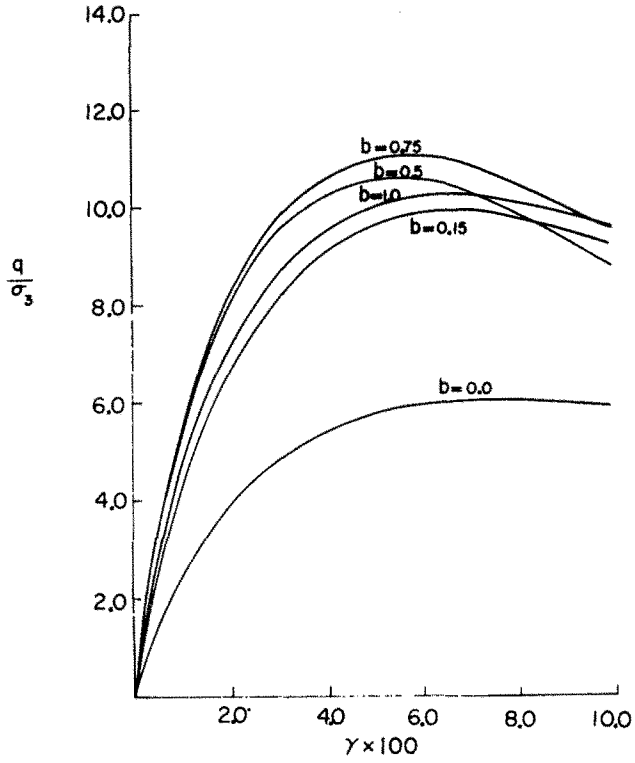

Fig. 18. Normalized shear stress, q/σ_3, as a function of the effective strain, γ: Parameters are the same as those for Figs. 6–10.

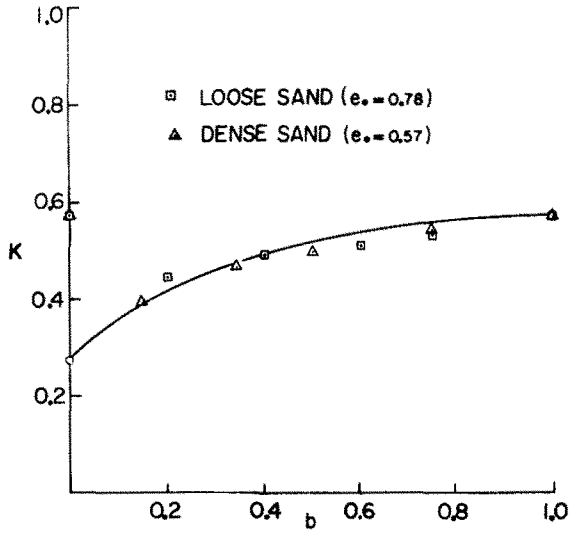

Fig. 19. Calculated values of K, based on experimental observation, for indicated true triaxial tests performed by Lade and Duncan[4] on Monterey No. 0 sand.

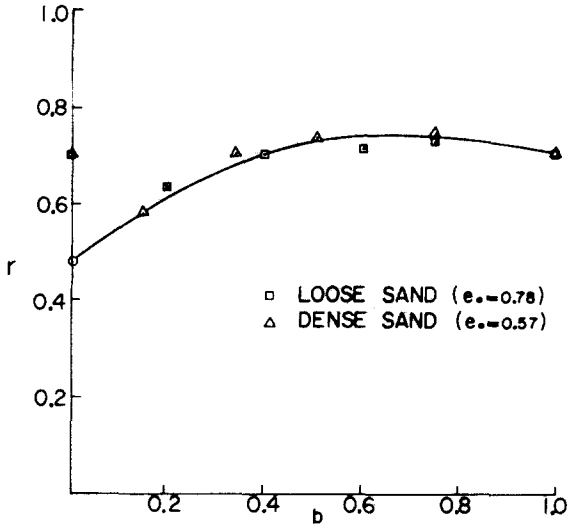

Fig. 20. Calculated values of r, based on experimental observation, for indicated true triaxial tests performed by Lade and Duncan[4] on Monterey No. 0 sand.

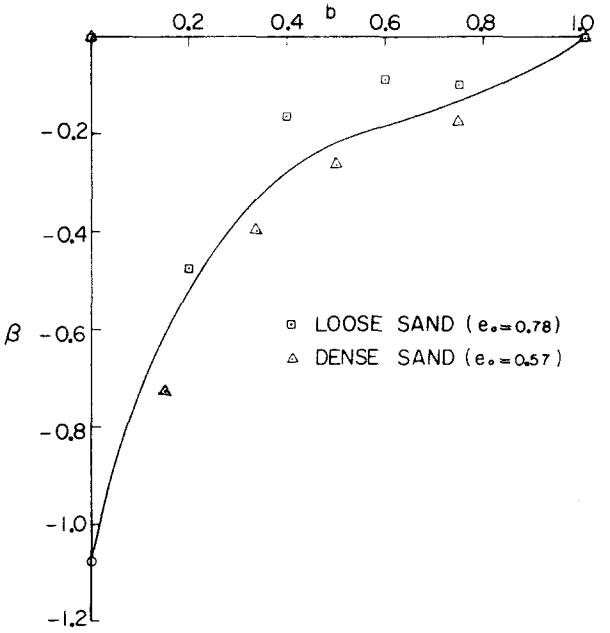

Fig. 21. Calculated values of β, based on experimental observation, for indicated true triaxial tests performed by Lade and Duncan[4] on Monterey No. 0 sand.

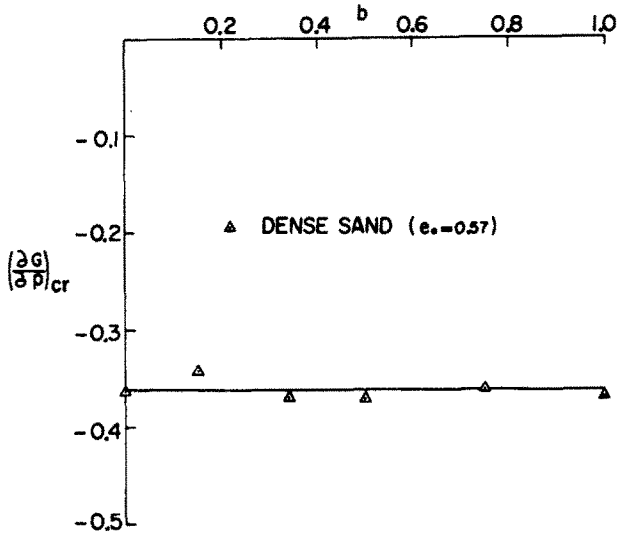

Fig. 22. Calculated values of dilatancy factor at peak strength, $(\partial G/\partial p)_{cr}$, based on experimental observation, for indicated true triaxial tests performed by Lade and Duncan[4] on Monterey No. 0 sand.

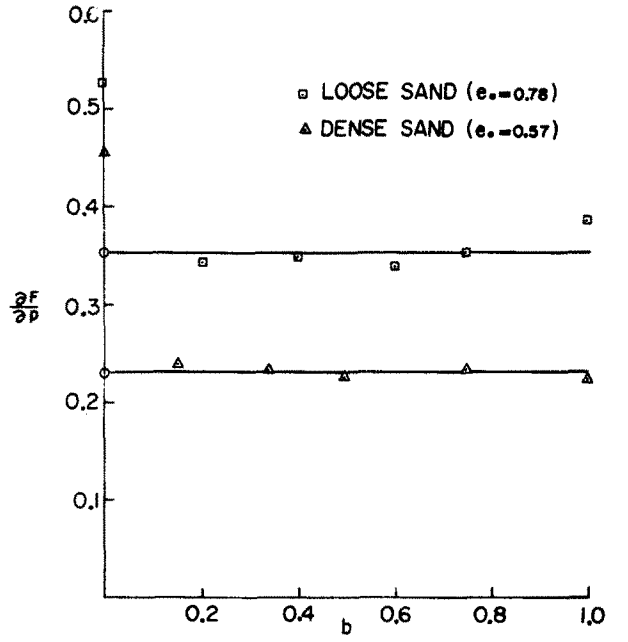

Fig. 23. Calculated values of $(\partial F/\partial p)$ based on experimental observation, for indicated true triaxial tests performed by Lade and Duncan[4] on Monterey No. 0 sand.

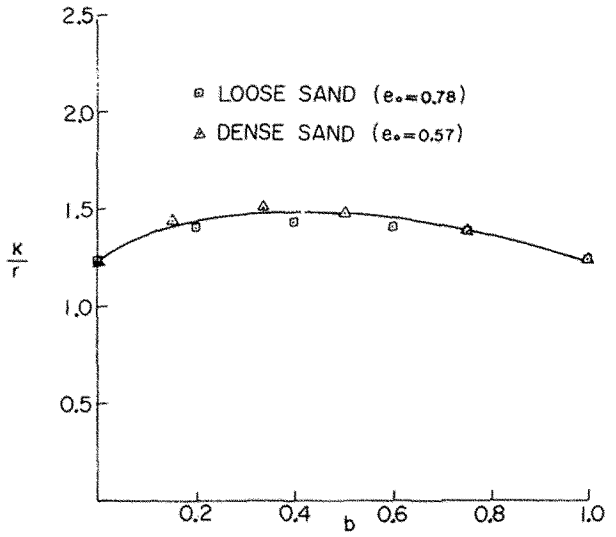

Fig. 24. Calculated values of (K/r), based on experimental observation, for indicated true triaxial tests performed by Lade and Duncan[4] on Monterey No. 0 sand.

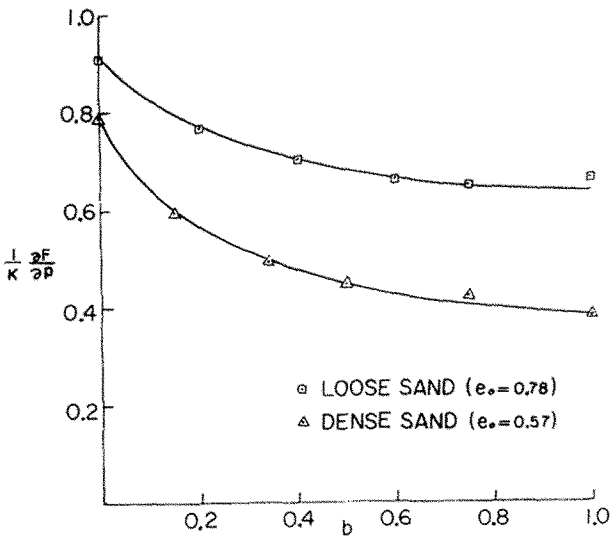

Fig. 25. Calculated values of $(1/K)(\partial F/\partial p)$, based on experimental observation, for indicated true triaxial tests performed by Lade and Duncan[4] on Monterey No. 0 sand.

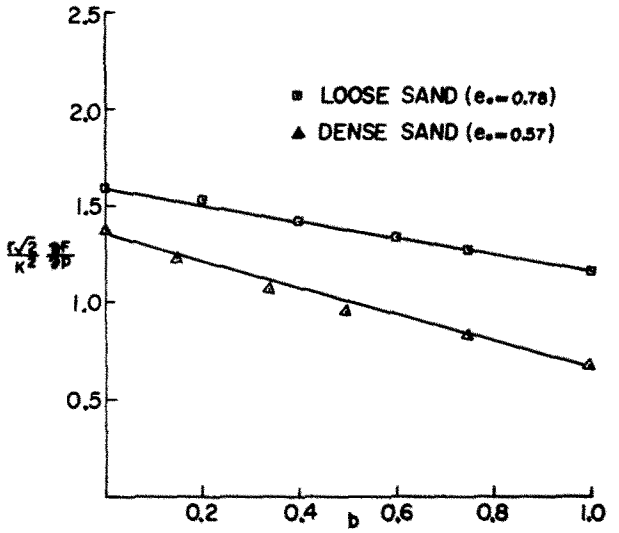

Fig. 26. Calculated values of $(r\sqrt{2}/K^2)(\partial F/\partial p)$, based on experimental observation, for indicated true triaxial tests performed by Lade and Duncan[4] on Monterey No. 0 sand.

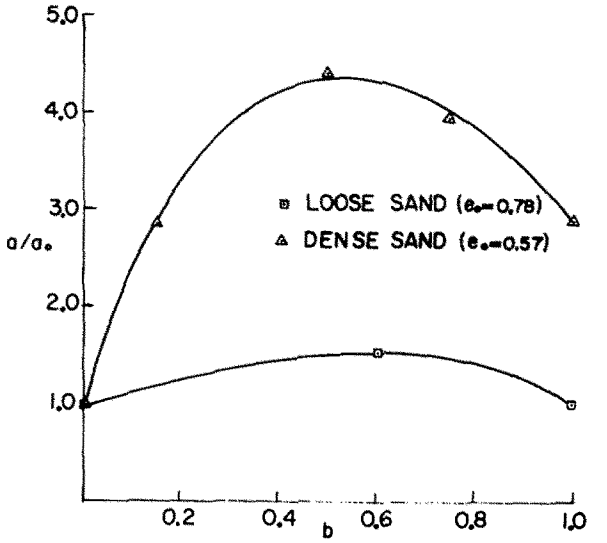

Fig. 27. Calculated values of the normalized coefficient of the density-hardening parameter, (a/a_o), for indicated true triaxial tests performed by Lade and Duncan[4] on Monterey No. 0 sand; a_o is the value of a at $b = 0$; $a_o = 14$ and 180 for dense and loose sands, respectively.

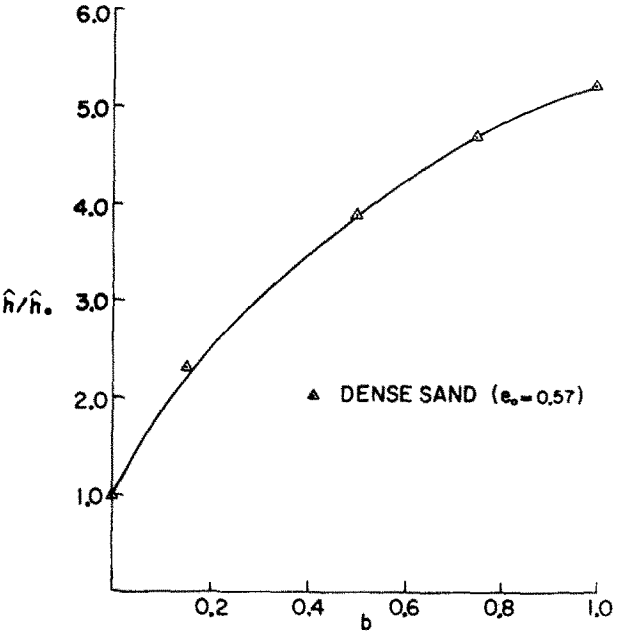

Fig. 28. Calculated values of the normalized coefficient of the distortional-hardening parameter, $(\hat{h}/\hat{h}_o)$, for indicated true triaxial tests performed by Lade and Duncan[4] on Monterey No. 0 sand; $\hat{h}_o$ is the value of $\hat{h}$ at $b = 0$; $\hat{h}_o = 430$ (dense sand).

(4) $(d\epsilon_{22}/d\epsilon_{11})$ and $(d\epsilon_{33}/d\epsilon_{11})$ are constants which depend on b; the data of Lade and Duncan[4] as well as the calculated strains in Figs. 11, 12, 16 and 17 show this to be a good approximation beyond 0.5% strain. Thus from (4.26), $(d\epsilon_{11}/d\gamma)$ is a constant which depends on b. The experimental data and the calculated curves show $(d\epsilon_{11}/d\gamma)$ to be an increasing function of b for a particular strain, and *for the sake of illustration we arbitrarily assume* $(d\epsilon_{11}/d\gamma) = 2.5b + 5$. It should be emphasized that this assumption is the only connection with experimental observation in this subsection.

(5) $(\partial F/\partial \Delta) = ap$. This assumption permits direct integration of $(4.25)_1$. The coefficient a is a positive constant for all b.

(6) $\beta = 0.0$. This assumption makes the differential equation independent of β and takes as the measure of distortional stress $J^{1/2}$ for all b. Dependence of the equation on b is maintained through the parameter K, the hydrostatic pressure, and $(d\epsilon_{11}/d\gamma)$.

(7) For the load path we assume σ_3 remains constant while σ_1 and σ_2 are increased in such a manner that b remains constant.

Utilizing these assumptions, normalizing with respect to σ_3, and integrating, we find

$$\bar{q}(\epsilon_{11}) = c_1(1 - e^{-c_2\epsilon_{11}}) + \frac{\hat{h}}{c_2 - \hat{\rho}}(e^{-\hat{\rho}\epsilon_{11}} - e^{-c_2\epsilon_{11}}), \tag{5.1}$$

where

$$c_1 = \frac{\dfrac{r\sqrt{2}}{K}\dfrac{\partial F}{\partial p}}{\left[K - \dfrac{1}{3}(b+1)\dfrac{r\sqrt{2}}{K}\dfrac{\partial F}{\partial p}\right]}, \qquad c_2 = \frac{aD\left[K - \dfrac{1}{3}(b+1)\dfrac{r\sqrt{2}}{K}\dfrac{\partial F}{\partial p}\right]}{3K\left[K - \dfrac{1}{3}(b+1)\dfrac{\partial F}{\partial p}\right]}.$$

Solution (5.1) contains *qualitatively* all of the characteristics commonly observed in the stress, strain-relation of cohesionless soils under monotone loading. For loose soils, the hardening due to density changes is very dominant so that $\hat{h}$ can be taken as zero. In this case, the solution increases monotonically and approaches from below the critical value, c_1, as shown by Curve 1 of Fig. 29. In dense soils the distortional hardening plays a more important role and

we take $\hat{h} \neq 0$. Differentiating (5.1) with respect to ϵ_{11}, one can find that the solution has a well defined maximum. Hence in this case the solution increases, passes through the critical state, reaches a maximum, and then decreases to approach asymptotically from above the critical value, c_1. This type of behavior is characteristic of dense soils and is shown by Curve 2 of Fig. 29.

Next we choose for illustration $a=0.5$, $\hat{h}=5.0$, $(\partial F/\partial p)=0.4$ and $\hat{\rho}=5.0$, and we calculate $\tilde{q}(\epsilon_{11})$. The calculated angle of friction is shown in Fig. 30 as a function of b. The resulting shear strength is seen to be higher than the strengths normally observed in sands, because of the arbitrary values assigned to the parameters. However there is *qualitative* agreement with some of the results presented in Fig. 1.

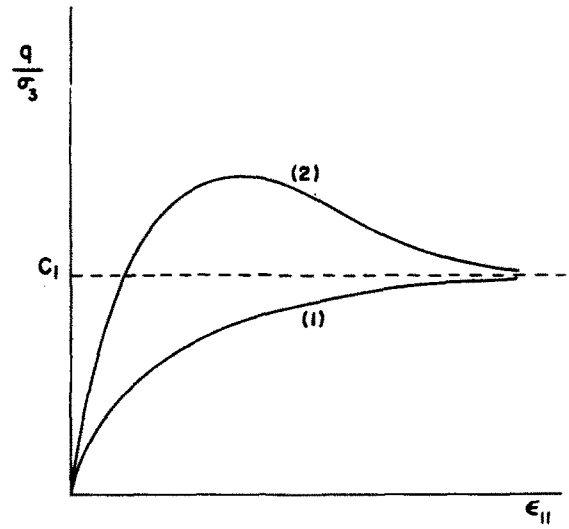

Fig. 29. Typical variation of the normalized differential stress, q/σ_3, with strain, ϵ_{11}; Curve 1 is for loose and Curve 2 is for dense samples.

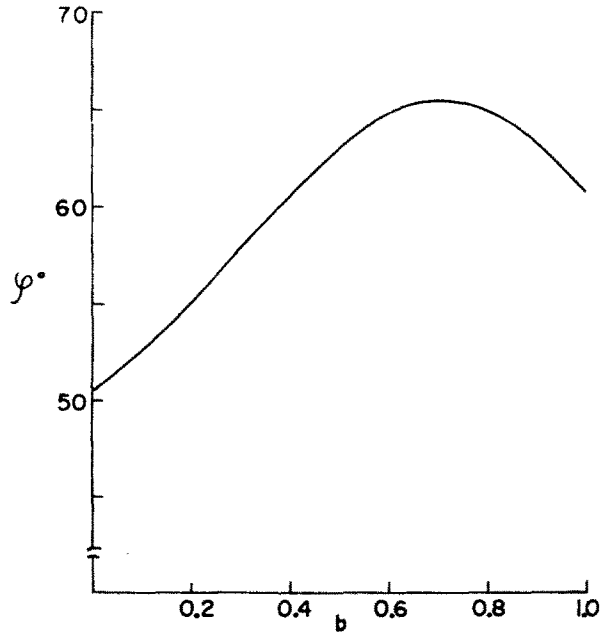

Fig. 30. Calculated angle of friction, ϕ, as a function of b; obtained from idealized assumptions for constitutive parameters.

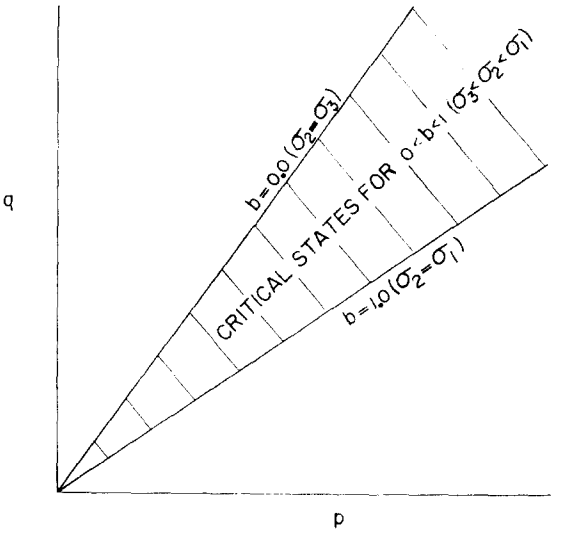

Fig. 31. Critical curves in the q, p-plane for true triaxial tests.

6. CONCLUDING REMARK

The preceding analysis develops a plasticity theory which includes the effects of pressure sensitivity, inelastic volume change, and internal friction for a general three-dimensional state of stress. Because of these effects the mechanical description of the behavior of granular materials is quite complex, and soil mechanics has traditionally simplified matters by presenting theories for two-dimensional states of stress which can easily be visualized and interpreted in the q, p-plane. The theory presented here follows this tradition since all results can also be presented in the q, p-plane. The important difference that separates this theory from others is that it allows for three-dimensional states of stress through the parameters r and K. Critical state soil mechanics, for example, defines a critical state in the q, p-plane which is valid for axially symmetric states of stress. Our theory, however, defines the critical state as $(q/p) = (r\sqrt{2}/K^2)(\partial F/\partial p)$ and if the results of Fig. 26 are plotted in the q, p-plane then we obtain a "wedge" of critical states. The wedge is bounded by the critical states for $b = 0$ and $b = 1$ and any line within the wedge defines the critical state for a particular σ_2 in the interval $\sigma_1 > \sigma_2 > \sigma_3$; see Fig. 31.

Acknowledgements—This work has been supported in part by the National Science Foundation under grant ENG 76-03921 and in part by U.S. Air Force Office of Scientific Research under grant AFOSR-80-0017 to Northwestern University.

REFERENCES

1. D. C. Drucker and W. Prager, Soil mechanics and plastic analysis of limit design. *Quart. Appl. Math.* **10**, 157–175 (1952).
2. W. M. Kirkpatrick, The condition of failure for sands. *Proc. 4th Int. Conf. on Soil Mechanics*, Vol. 1, pp. 172–178 (1957).
3. J. R. F. Arthur, T. Dunstan, Q. A. J. L. Al-Ani and A. Assadi, Plastic deformation and failure in granular media. *Géotechnique* **27**, 53–74 (1977).
4. P. V. Lade and J. M. Duncan, Cubical triaxial tests on cohesionless soils. *J. Soil Mech. Found. Div., ASCE* **99**, 793–812 (1973).
5. D. W. Reades and G. E. Green, Independent stress control and triaxial extension tests on sand. *Géotechnique* **26**, 551–576 (1976).
6. H. B. Sutherland and M. S. Mesdary, The influence of the intermediate principal stress on the strength of sand. *Proc. 7th Int. Conf. on Soil Mechanics*, Vol. 1, pp. 391–399 (1969).
7. G. E. Green, Strength and deformation of sand measured in an independent stress control cell. *Stress–Strain Behavior of Soils, Proc. of the Roscoe Memorial Symp.* (Edited by R. H. G. Parry), pp. 285–323. G. T. Foulis, Henley-on-Thames, England (1972).
8. S. Nemat-Nasser and A. Shokooh, On finite plastic flows of compressible materials with internal friction. *Int. J. Solids Structures* **16**, 495–514 (1980).
9. A. W. Bishop, The strengths of soils as engineering materials: 6th Rankine Lecture. *Géotechnique* **16**, 91–128 (1966).
10. J. Christoffersen, M. M. Mehrabadi and S. Nemat-Nasser, A micromechanical description of granular material behavior. Earthquake Research and Engineering Laboratory, Tech. Rep. 80-1-22, Dept. of Civil Engineering, Northwestern Univ. (Jan. 1980); *J. Appl. Mech.* **48**, 339–344 (1981).

11. S. C. Cowin and M. Satake (Eds), *Continuum Mechanical and Statical Approaches in the Mechanics of Granular Materials, Proc. U.S.-Japan Sem.* Gakujutsu Bunken Fukyukai, Tokyo (1978).
12. Y. F. Dafalias and E. P. Popov, A model for non-linearly hardening materials for complex loadings. *Acta Mechanica* **21**, 173–192 (1975).
13. G. de Josselin de Jong, *Statics and Kinematics in the Failable Zone of a Granular Material.* Uitgeverij, Delft (1959).
14. D. C. Drucker, R. E. Gibson and D. J. Henkel, Soil mechanics and work-hardening theories of plasticity. *Trans. ASCE* **122**, 338–346 (1957).
15. G. Gudehus, Elastoplastische stoffgleichungen für trockenen sand. *Ing. Archive* **42**, 151–169 (1973).
16. P. V. Lade, Elasto-plastic stress-strain theory for cohesionless soils with curved yield surfaces. *Int. J. Solids Structures* **13**, 1019–1035 (1977).
17. K. L. Lee and H. B. Seed, Drained strength characteristics of sands. *J. Soil Mech. Found. Div., ASCE* **93**, 117–141 (1967).
18. G. Mandl and R. Fernández Luque, Fully developed plastic shear flow of granular materials. *Géotechnique* **20**, 277–307 (1970).
19. M. M. Mehrabadi and S. C. Cowin, Initial planar deformation of dilatant granular materials. *J. Mech. Phys. Solids* **26**, 269–284 (1978).
20. Z. Mróz, On the description of anisotropic work-hardening. *J. Mech. Phys. Solids* **15**, 163–175 (1967).
21. Z. Mróz, V. A. Norris and O. C. Zienkiewicz, Application of an isotropic hardening model in the analysis of elasto-plastic deformation of soils. *Géotechnique* **29**, 1–34 (1979).
22. Z. Mróz and C. Szymanski, Non-associated flow rules in description of plastic flow of granular materials. *Limit Analysis and Rheological Approach in Soil Mechanics.* CISM Course 217, Udine, 1974, Springer Verlag (1979).
23. S. Nemat-Nasser, On behavior of granular materials in simple shear. *Soils and Foundations* **20**, 59–73 (1980).
24. J.-H. Prevost and K. Höeg, Effective stress–strain-strength model for soils. *J. Geot. Eng. Div., ASCE* **101**, 259–278 (1975).
25. J.-H. Prevost, Plasticity theory for soil stress–strain behavior. *J. Engng Mech. Div., ASCE* **104**, 1177–1194 (1978).
26. M. Romano, A continuum theory for granular media with a critical state. *Arch. Mech. Stos.* **26**, 1011–1028 (1974).
27. P. W. Rowe, The stress dilatancy relation for static equilibrium of an assembly of particles in contact. *Proc. R. Soc. (London)* **A269**, 500–527 (1962).
28. A. Schofield and P. Wroth, *Critical State Soil Mechanics.* McGraw-Hill, London (1968).
29. R. F. Scott and H.-Y. Ko, Stress deformation and strength characteristics. *Proc. 7th Int. Conf. on Soil Mechanics*, pp. 1–49 (1969).
30. A. J. M. Spencer, A theory of kinematics of ideal soil under plane strain conditions. *J. Mech. Phys. Solids* **12**, 337–351 (1964).
31. A. J. M. Spencer, Deformation of ideal granular materials. *Mechanics of Solids*, The Rodney Hill 60th Anniversary Vol. (Edited by H. G. Hopkins and M. J. Sewell), pp. 607–652, Pergamon Press, Oxford (1982).
32. P. A. Vermeer, A double hardening model for sand. *Géotechnique* **28**, 413–433 (1978).
33. P. Wilde, Two invariant dependent models of granular media. *Arch. Mech.* **29**, 799–809 (1977).
34. Z. Mróz, Deformation and flow of granular materials. *Theoretical and Applied Mechanics* (Edited by F. P. J. Rimrott and B. Tabarrok), pp. 119–132. North Holland, Amsterdam (1980).
35. C. A. Berg, Plastic dilation and void interaction. *Inelastic Behavior of Solids* (Edited by M. F. Kanninen *et al.*), pp. 171–209. McGraw-Hill, New York (1970).
36. J. W. Rudnicki and J. R. Rice, Conditions for the localization of deformation in pressure-sensitive dilatant materials. *J. Mech. Phys. Solids* **23**, 371–394 (1975).
37. K. Mogi, Fracture and flow of rocks. *Tectonophysics* **13**, 541–568 (1972).
38. S. Nemat-Nasser, On constitutive behavior of fault materials. *Solid Earth Geophysics and Geotechnology*, AMD-Vol. 42 (Edited by S. Nemat-Nasser), pp. 31–37. American Society of Mechanical Engineers, New York (1980).
39. R. Hill, A general theory of uniqueness and stability in elastic-plastic solids. *J. Mech. Phys. Solids* **6**, 236–246 (1958).
40. J. Mandel, Thermodynamics and plasticity. *Proc. Int. Symp. Foundations of Continuum Thermodynamics* (Edited by J. J. Delgado Domingos, M. N. R. Nina and J. H. Whitelaw), pp. 283–304. MacMillan, London (1974).
41. J. Mandel, Sur la définition de la vitesse de déformation élastique et sa relation avec la vitesse de contrainte. *Int. J. Solids Structures* **17**, 873–878 (1981).
42. S. Nemat-Nasser, Decomposition of strain measures and their rates in finite deformation elasto-plasticity. *Int. J. Solids Structures* **15**, 155–166 (1979).
43. R. Hill, *The Mathematical Theory of Plasticity.* Oxford University Press (1950).